

**Fatigue assessment of composite steel-concrete
cable-stayed bridge decks**

Maxime Bernard Duval

Thesis to obtain the Master of Science Degree in

Civil Engineering

Supervisors

Prof. Dr. José Joaquim Costa Branco de Oliveira Pedro

Prof. Dr. Alain Nussbaumer

Examination Committee

Chairperson: Prof. Jorge Miguel Silveira Filipe Mascarenhas Proença

Supervisor: Prof. Dr. José Joaquim Costa Branco de Oliveira Pedro

Members of the Committee: Prof. Francisco Baptista Esteves Virtuoso

June 2017

Acknowledgements

This Master thesis marks the end of an unpredictable journey through all these years of studies. It is a good conclusion of my Bachelor and Master degrees in the Civil Engineering section of the Ecole Polytechnique Fédérale de Lausanne. This project has allowed me to use and consolidate all the knowledge I have learned since the beginning. It has been a real pleasure to work on this project and all of this would not have been possible without the help and support of some people I would like to thank.

To Professors Alain Nussbaumer (EPFL) and José J. Oliveira Pedro (IST), for the opportunity they gave me to work on this project. Their support, their knowledge and all the time they have invested have been an invaluable help to me.

To Claudio Baptista, for all the energy he spent to explain me all small subtleties of fatigue verification procedures and of traffic generation. To André Biscaya, for his help, his availability and his kindness each time I had a question.

To Pierre Lorne, who shared with me this wonderful semester in Lisbon. For all the work we did together but also for all these crazy and incredible moments that made these months unforgettable.

To my parents, for their constant support, encouragement and patience. They have enabled me to reach higher objectives that I could not imagine.

To all of my friends, wherever they are, for all these moments spent to study, to have fun and to enjoy life. Thank you to them for these trips, these breaks and these party that made all these years of study the best memories ever. Finally, big up to Elodie Bisetti for being there with me since the beginning. A great thank you to her support, her laugh and her friendship!

Abstract

Fatigue safety verification is an important part in the steel highway and railway bridge design. The part 2 of the Eurocode 3 (EC3-2) proposes a simple and fast fatigue verification procedure. This one consists to determine a value of an equivalent stress range based on the passage of the vehicle FLM3, which is multiplied by a λ factor, called damage equivalent factor, and to compare it with the resistant stress range of each selected fatigue detail. However, λ factor has limits and it is not defined in the EC3-2 for some forms and lengths of influence lines. Cable-stayed bridges are precisely included in fields in which this procedure is not effective.

The objective of this Master thesis is to obtain the damage equivalent factor λ for cases, which are not valid in the EC3-2. In this content, an adjustment of the fatigue verification procedure will be proposed in order to allow for structural systems such as cable-stayed bridges to be taken into account.

Keywords

Cable-stayed bridge

Fatigue design

Fatigue load model

Influence line

Damage equivalent factor

Resumo

A verificação da segurança à fadiga é correntemente condicionante no dimensionamento de pontes rodoviárias e ferroviárias em aço. A parte 2 do Eurocódigo 3 (EC3-2) propõe um procedimento simples e rápido para a verificação da segurança à fadiga. Este consiste em determinar o valor de cálculo da amplitude de tensão nominal com base na passagem do veículo FLM3, multiplicado por um fator λ , denominado fator equivalente de dano, e compará-lo com o valor de tensão resistente, para cada detalhe de fadiga. No entanto, a utilização deste método está limitada no EC3-2 em termos da forma e comprimento da linha de influência, havendo casos em que esta metodologia não é directamente aplicável. Tal ocorre precisamente no caso de pontes de tirantes, onde o fator λ não é possível de obter pelo EC3-2.

O objetivo deste trabalho é obter directamente o fator equivalente de dano λ para as situações não contempladas no EC3-2. Dessa forma, complementa-se o procedimento de verificação à fadiga utilizando o método simplificado proposto no EC3-2, nomeadamente ao caso das pontes de tirantes.

Palavras-chave

Ponte de tirantes

Verificação da fadiga

Fator equivalente de dano

Modelo de carregamento de fadiga

Linha de influência

Contents

- 1. INTRODUCTION 1**
 - 1.1. GENERAL CONSIDERATION 1
 - 1.2. CABLE-STAYED BRIDGE DESIGN 5
 - 1.3. OBJECTIVES OF THE PROJECT 10
- 2. FATIGUE DESIGN IN STEEL STRUCTURES 13**
 - 2.1. MAIN PARAMETERS INFLUENCING FATIGUE LIFE 14
 - 2.2. FATIGUE CURVES & DESIGN 14
 - 2.3. DAMAGE EQUIVALENT FACTOR 17
 - 2.4. DAMAGE ACCUMULATION 20
 - 2.5. FATIGUE LOAD MODELS 21
- 3. MODELLING OF THE STUDY CASE 25**
 - 3.1. VASCO DA GAMA BRIDGE 25
 - 3.2. SAP MODELING 28
- 4. FATIGUE DETAILS 35**
 - 4.1. SELECTED DETAILS OF BOTTOM FLANGE 35
 - 4.2. SELECTED DETAILS OF STAYS 37
- 5. INFLUENCE LINES 39**
 - 5.1. STRESS INFLUENCE LINES OF BOTTOM FLANGE 39
 - 5.2. STRESS INFLUENCE LINES OF STAYS 41
- 6. FATIGUE ASSESSMENT OF BOTTOM FLANGE 45**
 - 6.1. VERIFICATION USING THE DAMAGE EQUIVALENT FACTOR 45
 - 6.2. VERIFICATION USING THE DAMAGE ACCUMULATION METHOD 47
 - 6.3. CONCLUSIONS 49
- 7. FATIGUE ASSESSMENT OF STAYS 51**
 - 7.1. VERIFICATION USING THE DAMAGE EQUIVALENT FACTOR 52
 - 7.2. VERIFICATION USING THE DAMAGE ACCUMULATION METHOD 52
 - 7.3. CONCLUSIONS 53
- 8. COMPARISON OF DAMAGE EQUIVALENT FACTORS 55**
 - 8.1. RESULTING FROM CODE LOAD MODEL 55
 - 8.2. RESULTING FROM SERVICE LOADS 56
 - 8.3. DAMAGE EQUIVALENT FACTOR 63

9. CONCLUSIONS AND FUTURE WORKS	69
9.1. STRESS INFLUENCE LINES	69
9.2. DAMAGE EQUIVALENT FACTOR.....	69
9.3. ADJUSTMENT OF THE EXISTING STANDARD RULES	70
9.4. FUTURE WORKS	70
REFERENCES	71
APPENDIX 1.....	73
CASE STUDY DETAILS	73
APPENDIX 2.....	75
STAYS TENSIONING	75
APPENDIX 3.....	77
SIMPLE INFLUENCE LINES FROM EN 1993-2 [7], ARTICLE 9.5.2 (2), AS FOLLOWS:.....	77
APPENDIX 4.....	79
INFLUENCE LINES OF LATERAL STAYS	79
APPENDIX 5.....	81
FATIGUE VERIFICATION PROCEDURES FOR STAYS	81

List of figures

- Figure 1.1 : The Lézardrieux bridge, 112m span (1925) 1
- Figure 1.2 : Brotonne bridge, 320m span (1977) 2
- Figure 1.3 : Alex Fraser bridge, 465m span (1986)..... 2
- Figure 1.4 : Normandie bridge, 856m span (1988) 3
- Figure 1.5 : Tatara bridge, 890m of span (1999)..... 3
- Figure 1.6 : Vasco da Gama bridge, 420m span (1998) 4
- Figure 1.7 : Millau Viaduct, 342m span (2004) 4
- Figure 1.8 : Fan and harp design..... 5
- Figure 1.9 : Semi-harp design 6
- Figure 1.10 : Forces transmission in cable-stayed bridge 6
- Figure 1.11 : Fan design vs Harp design 7
- Figure 1.12 : Utility of piers 7
- Figure 1.13 : Deformed structure under permanent loads..... 9
- Figure 1.14 : Axial forces diagram under permanent loads..... 9
- Figure 1.15 : Shearing forces diagram under permanent loads 9
- Figure 1.16 : Bending forces diagram under permanent loads..... 9
- Figure 2.1: Possible location of a fatigue crack in a road bridge (ECCS, 2011) [3]13
- Figure 2.2 : Fatigue strength curves for different detail categories (TGC 10, 2001) [2]15
- Figure 2.3 : Fatigue strength curves for tension components.....16
- Figure 2.4: Damage equivalent factor [3].....17
- Figure 2.5 : λ_{max} for road bridge [8]18
- Figure 2.6 : λ_1 for road bridge [8]19
- Figure 2.7 : Stress range histogram with S-N curve [2].....20
- Figure 2.8 : Fatigue load model 3 [3]21
- Figure 2.9 : Fatigue load model 4 [9]23
- Figure 3.1 : Vasco da Gama bridge25
- Figure 3.2 : Towers details [10]27
- Figure 3.3 : Vasco da Gama deck [10]28
- Figure 3.4 : Study case deck [10]28
- Figure 3.5 : Longitudinal configuration of the study case [10]29
- Figure 3.6 : Side view of the deck model30
- Figure 3.7 : Links between stays and towers31

Figure 4.1 : Typical FAT detail categories (SETRA [11]).....	35
Figure 4.2 : Stress variation in the main girder due to FLM3.....	36
Figure 4.3 : Selected elements of the main girder.....	36
Figure 4.4 : Details of the anchorage of the stays.....	37
Figure 4.5 : Table 9.1 of EN 1993-1-11 [6].....	38
Figure 5.1 : Influence lines of bottom flange elements.....	40
Figure 5.2 : Influence lines of lateral stays.....	41
Figure 5.3 : Influence line of L11.....	41
Figure 5.4 : Influence lines of central stays.....	42
Figure 7.1 : Comparison of Eurocode damage equivalent factor with FLM4 for long distance traffic.....	51
Figure 8.1 : CDF curve (from the software MatLab).....	57
Figure 8.2 : PDF curve (from the software MatLab).....	57
Figure 8.3 : Traffic generated (from the software MatLab).....	57
Figure 8.4 : Histogram for one-day data of stay C9.....	58
Figure 8.5 : Histogram for one-week data of stay C9.....	60
Figure 8.6 : One-day data vs one-week data of stay C1.....	61
Figure 8.7 : One-day data vs one-week data of stay C5.....	61
Figure 8.8 : One-day data vs one-week data of stay C13.....	62
Figure 8.9 : One-year data of stay C9.....	62
Figure 8.10 : Comparison of λ factors for C1, C5, C9 and C13.....	64
Figure 8.11 : Approximation of the lateral stay L7.....	66
Figure 8.12 : Comparison λ factors with $m=3,5$ and $m=4,6$	67

List of tables

Table 1 : Materials details.....31

Table 2 : Desired installed forces32

Table 3 : Calculated installed forces33

Table 4 : Critical length for elements of the bottom flange40

Table 5 : Critical lengths for stays.....43

Table 6 : Fatigue verification with FLM3 for element G446

Table 7 : Fatigue verification with FLM3 for the bottom flange47

Table 8 : Fatigue verification with FLM4 for element G448

Table 9 : Fatigue verification with FLM4 for the bottom flange48

Table 10 : Comparison damages for the bottom flange49

Table 11 : Fatigue verification with FLM3 for the stays52

Table 12 : Fatigue verification with FLM4 for stay L153

Table 13 : Fatigue verification with FLM4 for the stays53

Table 14 : Comparison damages for stays54

Table 15 : Stress range from load model.....55

Table 16 : Obtained results for one-day data of the stay C959

Table 17 : Obtained results for one-week data of the stay C9.....60

Table 18 : λ factors for the stays C1, C5, C9 and C1363

Table 19 : Comparison of λ factors for C1, C5, C9 and C1364

Table 20 : λ factors for m=3,5 and m=4,665

List of abbreviations and symbols

The following list is not exhaustive. Other notations may be introduced locally in the text.

Capital Latin letters

C	Constant representing the influence of the construction detail in fatigue strength expression
D, d	Damage sum, damage
M	Bending moment in Nm
N	Axial effort in N ; Number of cycles

Small Latin Letters

b_{eff}	Effective width of the concrete slab in m
m	Fatigue curve slope coefficient
n	Number

Capital Greek letters

$\Delta\sigma$	Stress range
$\Delta\sigma_B$	Total stress range considering the bending moment and the axial force
$\Delta\sigma_C$	Fatigue strength under direct stress range at 2 million cycles in N/mm ²
$\Delta\sigma_D$	Constant amplitude fatigue limit (CAFL) under direct stress range at 5 million cycles in N/mm ²
$\Delta\sigma_L$	Cut-off limit under direct stress range at 100 million cycles in N/mm ²
$\Delta\sigma_{E2}$	Equivalent direct stress range compute at 2 million cycles in N/mm ²

Small Greek letters

γ_{Ff}	Partial safety factor for fatigue action effects
γ_{Mf}	Partial safety factor for fatigue strength
λ	Damage equivalent factor
λ_1	Factor accounting for span length (in relation with the length of the influence line)
λ_2	Factor accounting for a different traffic volume than given
λ_3	Factor accounting for a different design working life of the structure than given
λ_4	Factor accounting for the influence of more than one load on the structural member
λ_{max}	Maximum damage equivalent factor value, taking into account the fatigue limit

1. Introduction

1.1. General consideration

Cable-stayed bridges are new and elegant structures. For the last 30-40 years, construction of cable-stayed structures has been developed rapidly with span record and important technological advances and today it is considered as the most modern structural system for bridge. Nowadays, concrete and steel, the two most popular materials in the constructions, are used in an optimal way to have more economic structures.

First cables were used for suspended bridges. But then engineers had the idea to use them as stays. The first cable-stayed bridges were built in the beginning of the 19th century, but collapsed such as on the Tweed in 1818 and on the Saale in 1824. The main reasons were that engineers didn't know well how the forces transmission was made and what the effects of the winds were.

This system was then absolutely discredited and it took a hundred years for engineers to try the cable-stayed systems again. The Lézardrieux bridge, built in 1925 with a 112m central span, could be also considered as the first cable-stayed bridge (Virlogeux, 2002) [1].



Figure 1.1 : The Lézardrieux bridge, 112m span (1925)¹

Its main characteristic is that the central stays are crossing. The deck is in concrete and there were some modifications made on this bridge such as increasing the deck's width.

¹ <https://files1.structurae.de/files/photos/1/100km023/pict7475.jpg>

The first major development in the cable-stayed bridges was the use of concrete. German engineers became the leaders in 1955 during several years. In the end of the 1970's, cable-stayed bridges design became international and it is Japan who took then the leadership of this type of construction. As an example, the Brotonne bridge which was built in 1977 with a deck made entirely in concrete.



Figure 1.2 : Brotonne bridge, 320m span (1977)²

It was the record span for concrete bridges of all types at that time with a 320m central span. Furthermore, the engineers began using widely distributed multiples stays.

The second evolution was the use of composite steel-concrete bridge decks. This development allowed the cable-stayed bridges to enter in the search of the greatest span. Indeed, the use of the two materials had as consequences to obtain more lightweight and more resistant structures, such as the Alex Fraser Bridge, built in Canada in 1986 with a 465m span. its deck is composed by two main steel girders with I-shape and precast concrete slab on top.



Figure 1.3 : Alex Fraser bridge, 465m span (1986)³

² <https://files1.structurae.de/files/photos/618/bretonnes1.jpg>
³ <https://files1.structurae.de/files/350high/wikipedia/AlexFraserBridge.jpg>

Then occurred an explosion of constructions, with a couple of structures that may compete with other bridge systems, as suspension bridges, for the longest bridge in the world, such as the Normandie bridge, built in 1988 in France with an 856m central span, and the Tataru bridge, built in 1999 in Japan with an 890m span.

Today we can consider several solutions to build the deck in an economic way such as: using prestressed concrete for 500-600m of span or composite steel-concrete deck for 700-800m of span or also orthotropic box for longer spans [1].



Figure 1.4 : Normandie bridge, 856m span (1988)⁴



Figure 1.5 : Tataru bridge, 890m of span (1999)⁵

⁴ <http://www.lamanchelibre.fr/photos/maxi/154059.jpg>

⁵ <http://www.irhal.com/image/stories/category/tallest/Worlds-Tallest-Bridges/Tataru-Bridge.jpg>

Actually, the world's longest cable-stayed bridge is the Russky bridge, in Russia. It was built in 2012 and its central span measures 1104m.

In the latest years, the deck's conception has evolved by using slim composite steel-concrete deck. This deck is usually composed of two longitudinal girders on the external sides, with a decreased height and low inertia, several steel transverse bracing frames and a precast concrete slab panel. Vasco da Gama bridge is a good example.



Figure 1.6 : Vasco da Gama bridge, 420m span (1998)

Finally, last important point is the case of multiple-span cable-stayed bridges. In fact, the stays create bending in the towers, which is taken up by the lateral span. If a tower is between two cable-stayed spans, there is nothing to avoid its flexion, thus the tower needs to be stiff. The Millau Viaduct, in France, is a good example. It was built in 2004 and its spans all measure 342m. It is a composite steel-concrete deck and has the highest piers-tower in the world, with a height of 343m. The proposed solution to prevent flexion is to increase the tower's bending stiffness with an A-shape, still allowing for longitudinal deformations with a low shear stiffness.



Figure 1.7 : Millau Viaduct, 342m span (2004)⁶

⁶ <https://upload.wikimedia.org/wikipedia/fr/a/a6/ViaducdeMillau.jpg>

1.2. Cable-stayed bridge design

The next explanations are mainly based on the chapter 10 (Ponts haubanés) of the EPFL course "Ponts en béton" of the Professor Aurelio Muttoni, especially the figures.

In this part, it will be explained the design of cable-stayed system. First of all, we need to understand how this system works and how the forces are transmitted. To do so, some schemes are described to explain the system's behavior. There are several types of cable-stayed systems: mono, harp, fan and star design. The two main types are the fan design and the harp one.

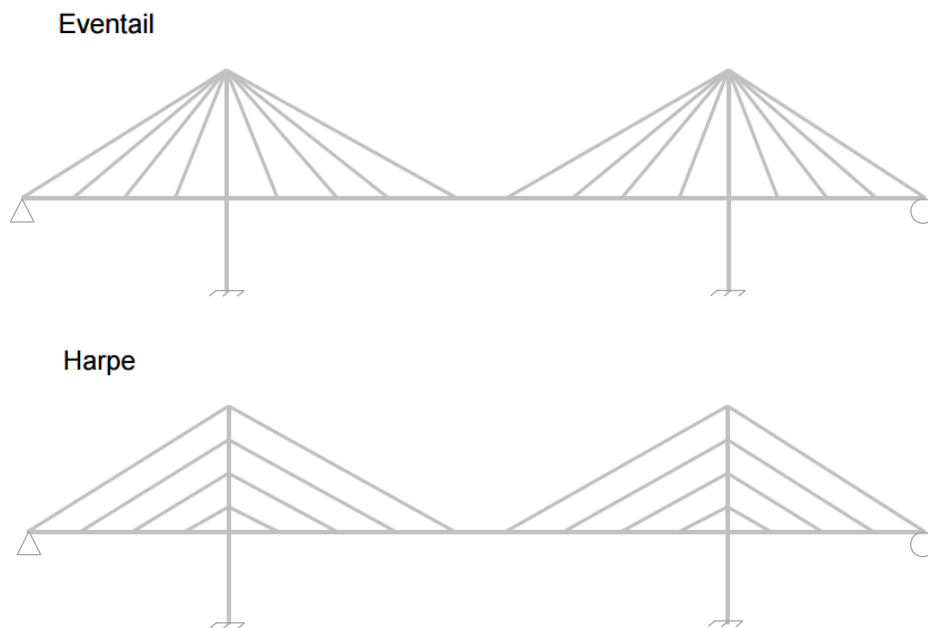


Figure 1.8 : Fan and harp design

The fan design is better from a static perspective. But, there is a construction problem to fix all the stays, especially if there are many. The harp design doesn't have this problem because the spans are distributed on the all tower's height. This design is more elegant and has a better visibility from a esthetic point of view. But this static system induces a greater compression in the deck than the fan design.

So one solution is to combine these two design. This solution is called the semi-harp design and it allows to solve the construction problem without excessively increasing the compression in the deck.

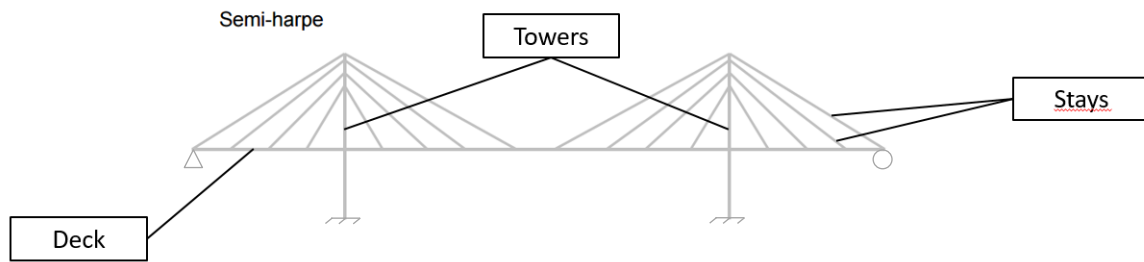


Figure 1.9 : Semi-harp design

Generally, there is traction in the stays and compression in the towers and the deck. To better understand, the Figure 1.10 shows how the forces are transmitted if only the external stays are considered.

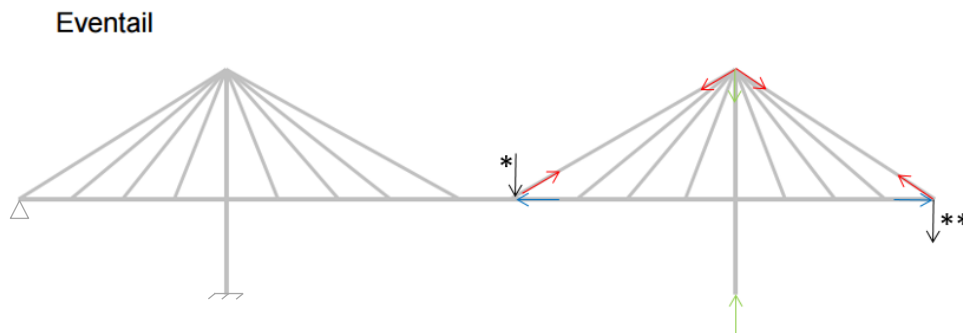


Figure 1.10 : Forces transmission in cable-stayed bridge

If the central span is loaded (black arrow *), it induces tension in the stay. To equilibrate it, the deck need to be compressed. Then, as the central stay is in traction, the lateral one need to be in traction too to balance the forces. This creates a high compression in the tower, which is transmitted to the ground. Finally, with the lateral stay in traction and the deck in compression, the forces must be transmitted to the ground (black arrow **) if we do not want an uplift of the end support.

Another important point: there is no need for connections between the deck and the tower. The deck is entirely supported by the stays, which transmit the forces in the tower. Then, considering all the stays in the Figure 1.11, it is possible to explain the difference between the harp and fan design from a static perspective.

For the fan design, we consider the resultant of the load (black arrow). It induces traction in the central stays and activates all lateral stays. The resultant of central stays is a vector directed towards the top of the tower, because it is the common point of all the stays. This involves a high angle with the horizontal plan and thus, to equilibrate the forces a compression appears in the deck (blue arrow).

Considering the harp design, the resultant of the central stays is directed to the middle of the tower and this involves an angle lower than the fan design. So the compression created in the deck is higher, but this also involves that the top part of the pylon is less loaded.

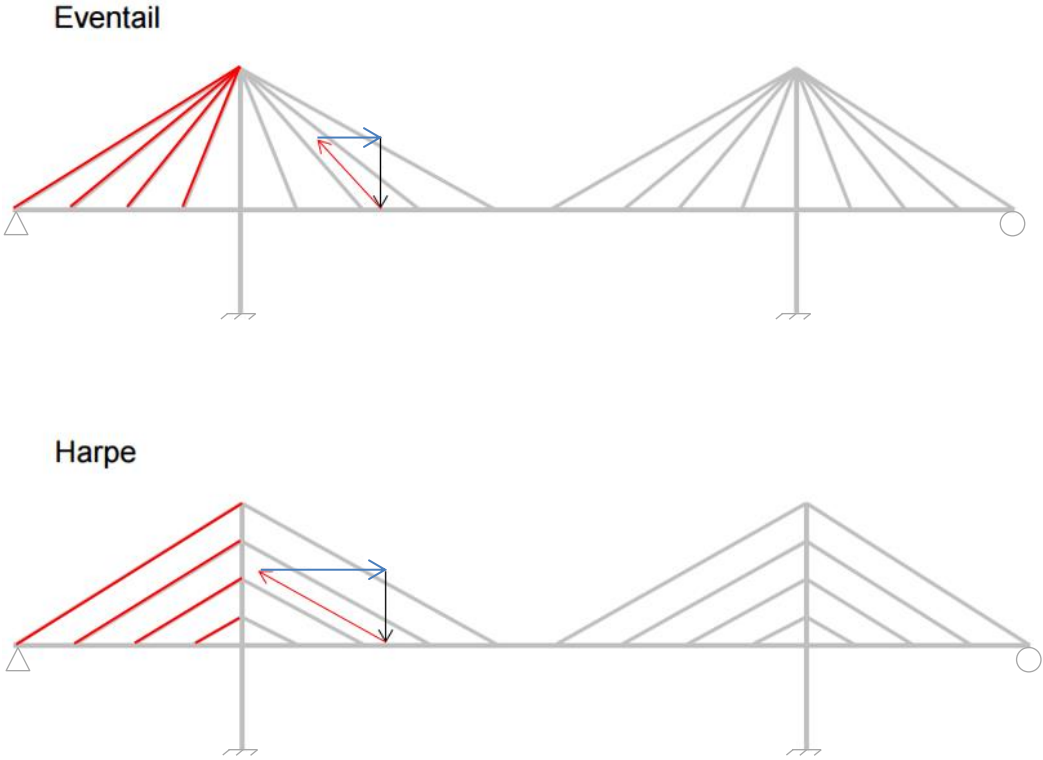


Figure 1.11 : Fan design vs Harp design

The next point to mention is the utility of the piers in the lateral spans. Indeed, considering the Vasco da Gama bridge as an example, one can notice three piers in each lateral span. By using them, it is possible to prevent flexion in the towers and incidentally in the deck, as described in the Figure 1.12.

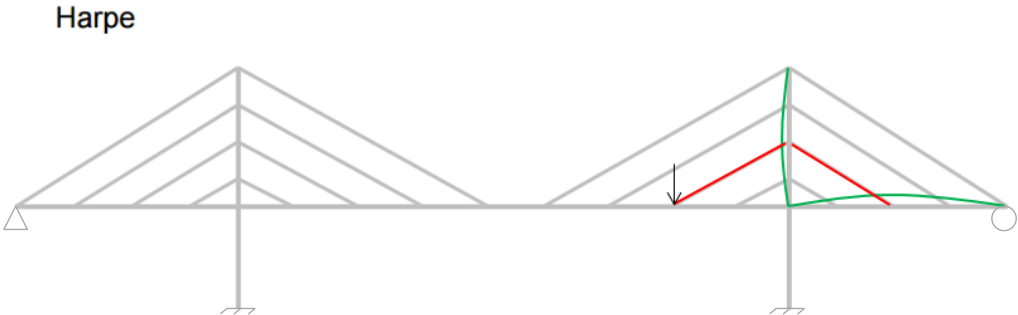


Figure 1.12 : Utility of piers

If the central span is loaded, this activates mainly the closest stay, which activate the one in the lateral span. The traction in the stay creates flexion in the deck and so induces flexion in the tower. The lateral supports take the flexion of the deck and allow to limit the tower top displacement and thus, to limit bending in the pylon.

To explain the behavior, the following figures come from the modelling made with the software SAP 2000. The deformed structure and all diagrams are considered under permanent loads, which is composed of the dead load of the supporting structure and the equipment, and the tension in the stays, which is explained later with all information of the modelling.

The main characteristic of the cable-stayed structure is that the stays induce compression in the deck. So there is a combination of two internal forces in the deck: flexion and compression. The stays, made of steel, are working only in traction and so cannot absorb flexion. The towers are massive structures made of concrete and need to absorb the important compression induced by the stays and so mainly work in compression.

In the figures below, the traction in each stay is much lower than the compression of the deck or the towers because of their number. Moreover, if the structure is symmetric, the axial force is null in the central space (between the two last stays). The compression in the deck first increases with each stay and after the tower, it decreases in a symmetric way.

A symmetry in the repartition of the shearing and bending forces is showed too (Figure 1.15 and Figure 1.16). As expected from the modelling assumption of reality, there are no shearing forces and no flexion in the stays.

For the shearing forces diagram, it is interesting to notice that the middle support in each lateral span, due to the piers, holds back the deck. The diagram is linear and the vertical component of each stay creates a bounce as we can see. For the bending forces diagram, it is parabolic with no or very small bending moment in the tower and it is similar to the deformed structure (Figure 1.13).

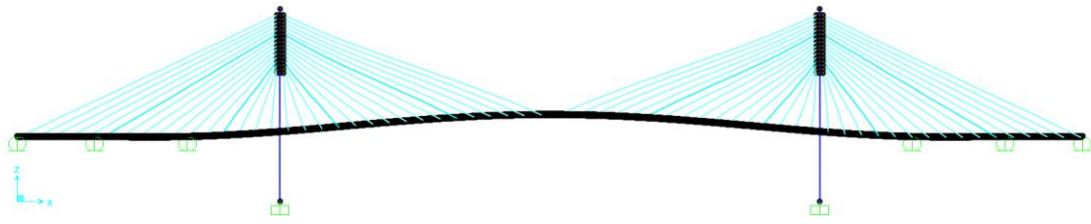


Figure 1.13 : Deformed structure under permanent loads

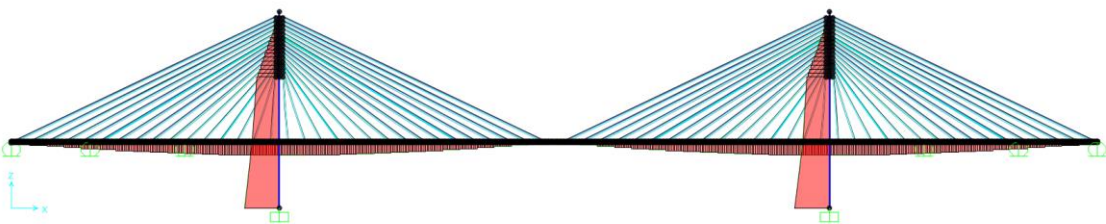


Figure 1.14 : Axial forces diagram under permanent loads

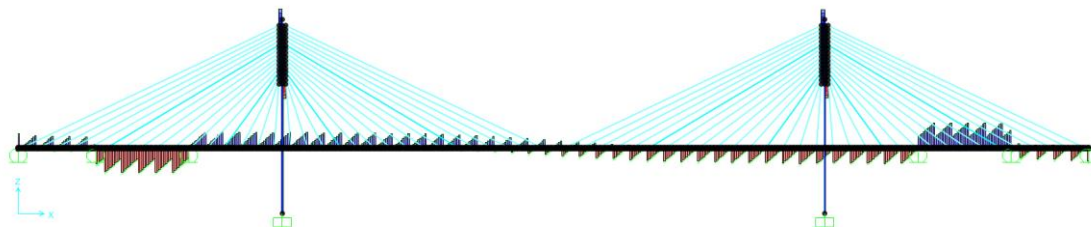


Figure 1.15 : Shearing forces diagram under permanent loads

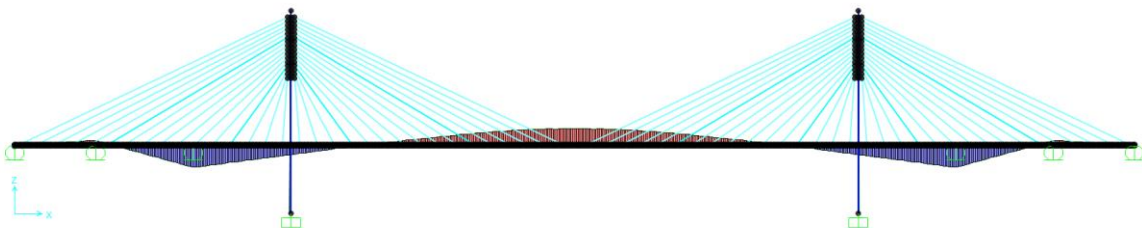


Figure 1.16 : Bending forces diagram under permanent loads

1.3. Objectives of the project

With this introduction as a better understanding of the cable-stayed system, this thesis will focus on the fatigue verification procedures for a cable-stayed bridge. The two procedures as described in the Eurocodes are the damage equivalent factor method and the damage accumulation method. The first one is based on a parameter, noted λ factor, which depends on the critical length of the influence line loaded. However, this λ factor is not calibrated for critical lengths higher than 80 m.

Moreover, influence lines of cable-stayed bridge may be very complex and can have critical lengths much higher than 80 m. Indeed, as explained previously, cable-stayed system is a structural system composed by two internal forces: bending moment and axial force. These two forces involve two different influence lines and it is not clear which one is the best to describe the maximum and minimum stresses. Stress influence lines must be defined to solve this problem in order to combine both of influence lines.

For this project, the Eurocodes which will be used to understand and perform the verification procedures are:

- *EN 1991-2*: Actions on structures – Part 2: Traffic on bridges
- *EN1993-1-9*: Design of steel structures – Part 1-9: Fatigue
- *EN1993-1-11*: Design of steel structures – Part 1-11: Design of structures with tension components
- *EN1993-2*: Design of steel structures – Part 2: Steel bridges

The main softwares which will be used are:

- *SAP 2000* for modelling and calculating the study case and the internal forces. It also helps to define the influence lines of the selected elements.
- *MatLab* for generating all traffic data and histograms and calculating the new damage equivalent factors.

The main objectives of this project have been defined at the beginning of the work as follows:

- Identification of fatigue details of composite decks to be analysed
- Modelling the cable-stayed bridge to obtain the important deck stress ranges
- Obtain stress influence lines and perform the fatigue verifications for the important details using two procedures
- Propose a fatigue verification procedure based on the adjustment of the existing standard rules

In this context, the project is divided into nine chapters. First of all, all the theoretical points related to the fatigue verifications will be described. The third chapter will concern all the information about the case study and the modelling. Then, the fatigue details will be selected in order to perform the verifications and the influence lines associated to these details will be determined.

On the basis of all this information, the fatigue assessment will be performed on some elements of the main steel girder and on some stays. In the last chapter, new damage equivalent factors will be evaluated for critical lengths higher than 80 m and an adjustment of the standard rules of the Eurocodes will be proposed.

2. Fatigue design in steel structures

With this chapter I want to explain the theoretical points related to this project. To do so, I take a great inspiration of the “Traité de Génie Civil, Vol. 10” (TGC 10, 2001) [2] and of the “ECCS Eurocode design manuals” (ECCS, 2011) [3] in order to have a correct theoretical base to understand fatigue. A synthesis is done, which includes some Eurocode’s articles.

Fatigue is one of the main causes of damage in steel structures and occurs when members, connections or joints are subjected to repeated cycling loadings such as road and rail traffic. These actions develop cracks in the material and may cause crack propagation in the steel element and progressive damage in the time until this one breaks due to a loss of resistance.

After a lot of researches in the fatigue resistance area, it has been demonstrated that geometrical changes, stress concentration and discontinuities are origins of the formation and propagation of cracks. That means that particular places can be identify where fatigue problems appear. Thus, the connections and/or joints in steel structures are the critical places for the fatigue cracking. Figure 2.1 shows a good example of a composite road bridge deck subjected to cycling loading where geometrical changes of gusset induce stress concentrations and so fatigue cracking near to the weld.

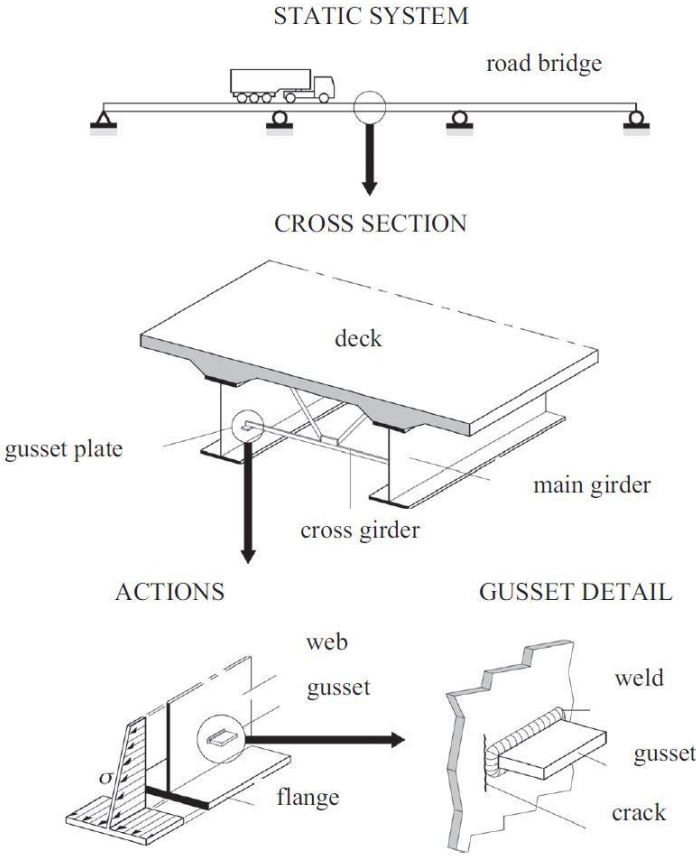


Figure 2.1: Possible location of a fatigue crack in a road bridge (ECCS, 2011) [3]

The purpose of this first chapter is to explain the parameters influencing the fatigue life and the different procedures for the fatigue design of road bridges.

2.1. Main parameters influencing fatigue life

Fatigue life of steel members, connections or joints is defined by the number of cycle that the element can support before it fails. There are four main parameters that influence fatigue resistance.

The first one is the more important and the more influent parameter. It is the stress variation, or also called the stress range (defined by the equation (2.1)). It can be calculated using the difference between the maximum stress value in the steel element and the minimum one (with sign).

$$\Delta\sigma = \sigma_{max} - \sigma_{min} \quad (2.1)$$

Another parameter is the geometry of the detail. Indeed, this one is essential for the location of the fatigue crack and hence directly influences the fatigue life of the member. As an example, a sharp geometrical change rises the stress flow and, thus, the fatigue resistance of the structural detail, using gussets, welds or section changes, can be improved with a good design.

The third parameter is related to the material characteristics. It has been observed during fatigue test that mechanical characteristics may enhance the fatigue life, especially on the crack initiation phase. Indeed, better material characteristics increase the time required to initiate the crack.

Finally, the last one concern the influence of the environment on the fatigue resistance of the steel member and in particular on the crack propagation phase. A humid and corrosive environment can, in fact, increase the crack propagation's rate and it is also necessary to use appropriate protections to get a better structural fatigue strength.

2.2. Fatigue curves & design

With the objective to evaluate fatigue resistance easily, standard curves (or S-N curves) have been created for different connections. These connections can be classified with the FAT, or also called $\Delta\sigma_c$, that represents the maximum stress range at 2×10^6 cycles, and are categorized in the tables 8.1 to 8.10 of the EN 1993-1-9 [4]. These curves are useful to verify that stress variation is lower than the limit and have also been determined with fatigue tests in which specimens are subjected to repeated cyclic loading with a constant stress range. The results are showed in the Figure 2.2 with the number of cycle (N) on the abscissa and the stress range ($\Delta\sigma$) on the ordinate. Thus, there is one fatigue curve for each detail category and these curves are also described with the following expression:

$$N = C \cdot \Delta\sigma^{-m} \quad (2.2)$$

where m is the slope coefficient and C is a constant representing the influence of the structural detail.

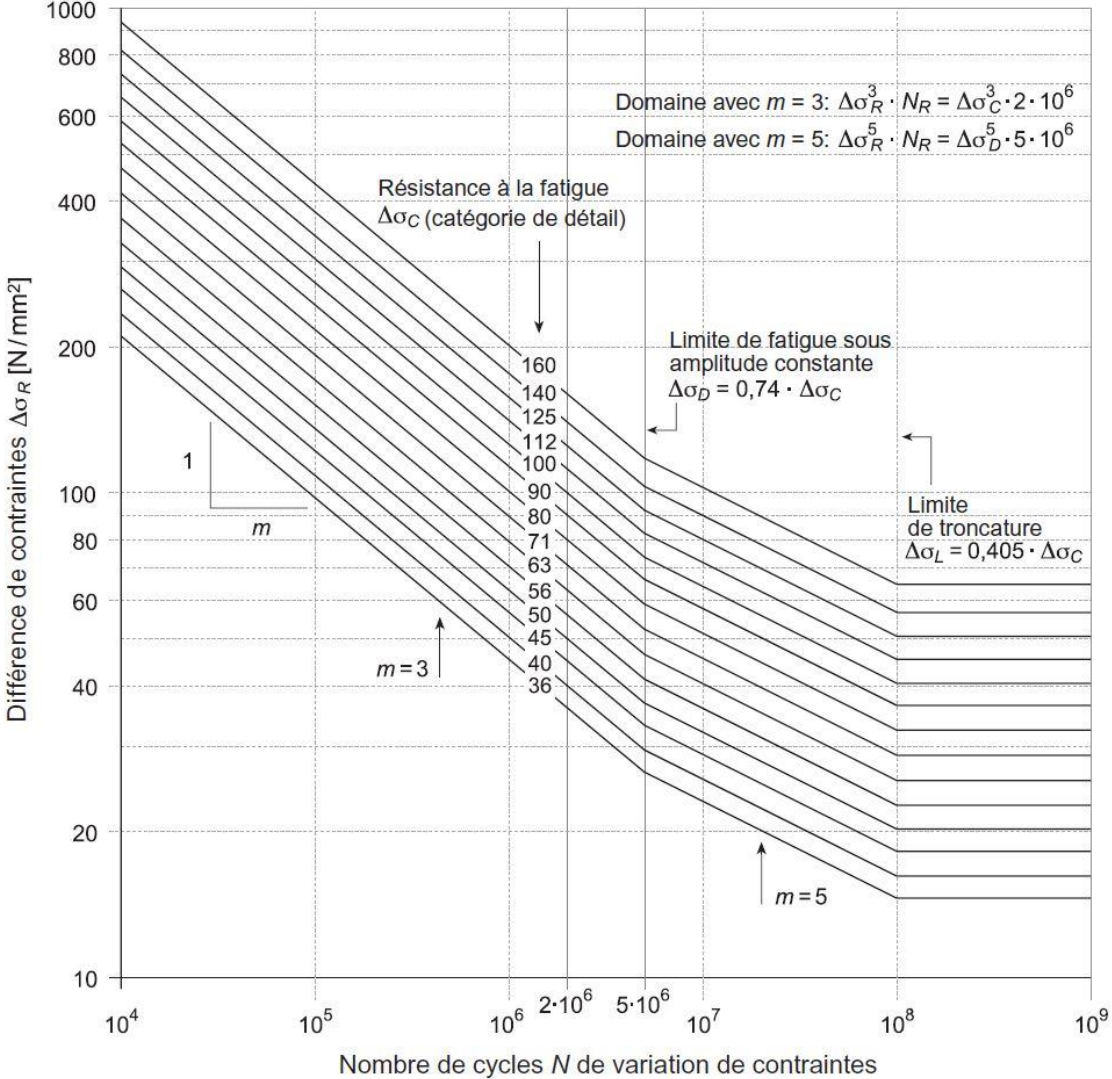


Figure 2.2 : Fatigue strength curves for different detail categories (TGC 10, 2001) [2]

Moreover, these fatigue curves can be decomposed into three different parts. The limited life part, where stress range corresponds to cycles between 10^4 and 5×10^6 . The stress range at 5×10^6 cycles being called CAFL (Constant Amplitude Fatigue Limit). S-N curve has a slope coefficient of 3 in the first part, i.e. if the stress range is higher than CAFL. The second part is between 5×10^6 and 10^8 , with a slope coefficient of 5. Then, 3rd part, higher than 10^8 cycles, there is the cut-off limit ($\Delta\sigma_D$) where stress variations under this limit may be completely neglected in damage accumulation (Maddah, 2013) [5].

Figure 2.2 concern the fatigue strength of steel element, but in this project stays are very important. After some researches about them, it has been demonstrated that fatigue strength for tension components have a different behaviour than other steel elements. This behaviour is defined in the Figure 2.3, taken from the EN 1993-1-11 [6].

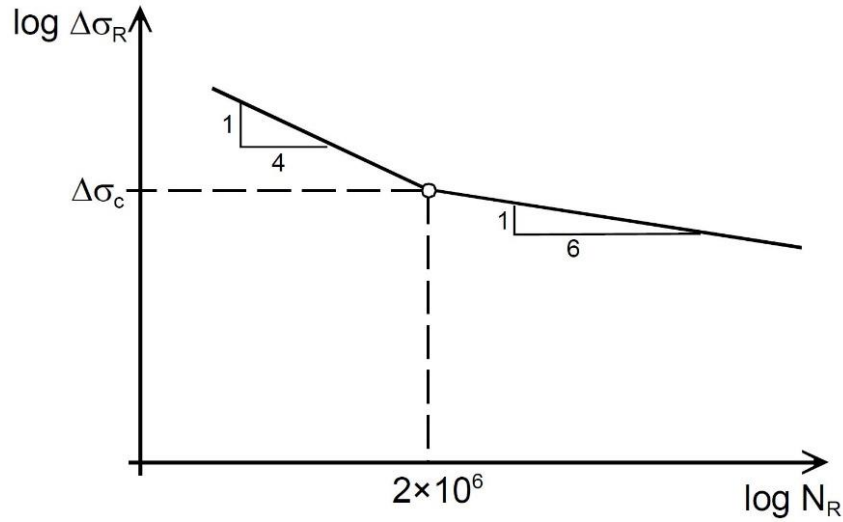


Figure 2.3 : Fatigue strength curves for tension components

There are only two parts in the Figure 2.3, separated by the stress range at 2×10^6 cycles ($\Delta\sigma_c$) and it is equal to 160 N/mm². The slope coefficients are equal to 4 for low cycles and 6 if the cycles are higher than 2×10^6 . Moreover, there is no cut-off limit and hence all stress range are taken into damage accumulation calculations.

Using fatigue curves, procedures related to the fatigue design can be described. Fatigue verifications are similar to the structural verifications and consist to verify that all traffic load effects are lower than the resistance of the bridge, as defined in the following relation:

$$E_d \leq R_d = \frac{R_{fat}}{\gamma_{Mf}} \quad (2.3)$$

or using the expressions in the article 9 of the EN 1993-2 [7]:

$$\gamma_{Ff} \cdot \Delta\sigma_{E2} \leq \frac{\Delta\sigma_c}{\gamma_{Mf}} \quad (2.4)$$

$$\Delta\sigma_{E2} = \lambda \cdot \Phi_2 \cdot \Delta\sigma \quad (2.5)$$

$\Delta\sigma_{E2}$ is the damage equivalent stress range at 2×10^6 cycles and must be calculated with the damage equivalent factor λ . Then, Φ_2 represents the damage equivalent impact factor and may be taken as equal to 1.0 for road bridges. Finally, two partial safety factors must be taken into account and are:

- γ_{Mf} for the fatigue action effects and is equal to 1.0
- γ_{Ff} for the fatigue strength and is equal to 1.35 in this project, as recommended in the table 3.1 of the EN 1993-1-9 [4]

2.3. Damage equivalent factor

The damage equivalent factor method is an easy and simplified way to get fatigue verifications with the damage equivalent stress range related to 2×10^6 cycles and, thus, avoid the damage accumulation calculations. The λ factor is obtained by the division between the stress variations due to a fatigue load model, usually FLM3, and the ones due to a real traffic. Figure 2.4 shows this procedure which will be explained more fully later in this report.

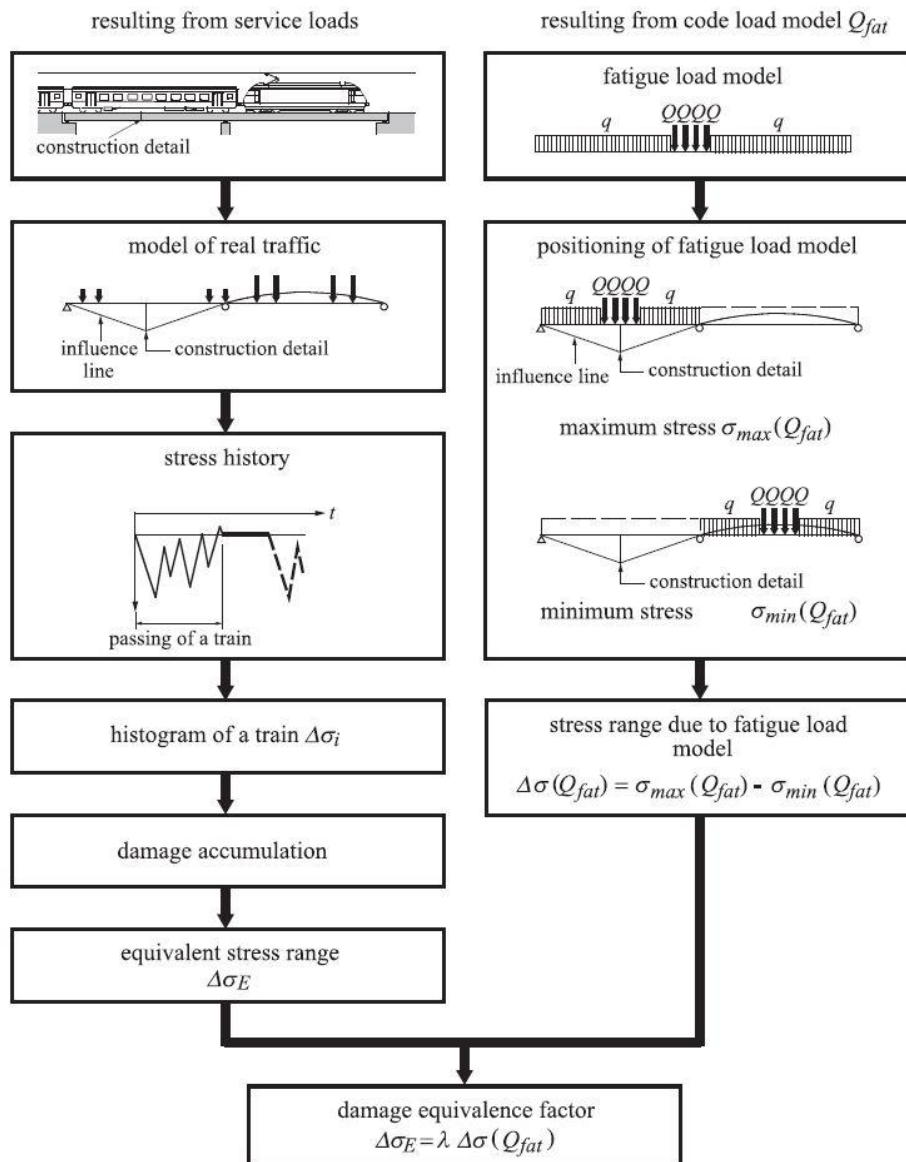


Figure 2.4: Damage equivalent factor [3]

The damage equivalent factor λ can be calculated according to the article 9.5.2 in the EN 1993-2 [8]:

$$\lambda = \lambda_1 \times \lambda_2 \times \lambda_3 \times \lambda_4 \leq \lambda_{max} \quad (2.6)$$

It is the product of four partial factors to take into account characteristics such as the composition and volume of the traffic or the working life of the bridge. A limit was also put with the factor λ_{max} that represents the maximum damage equivalent value and allows to avoid that the multiplication of the individual partial factor may result in a value far exceeding the one obtained from a design using fatigue limit [3]. This maximum value depends on the critical length of the influence line (L_{crit}) and the type of section. The importance and the value of the critical length are explained in the chapter 5. As described in the EN 1993-2 [8] and summarized in the Figure 2.5, the maximum value should be calculated as follows:

- at midspan section:

$$\begin{aligned}
 L_{crit} < 25m : & \quad \lambda_{max} = 2.5 - 0.5 * \frac{L_{crit} - 10}{15} \\
 L_{crit} \geq 25m : & \quad \lambda_{max} = 2.0
 \end{aligned}
 \tag{2.7}$$

- at support section:

$$\begin{aligned}
 L_{crit} < 30m : & \quad \lambda_{max} = 1.80 \\
 L_{crit} \geq 30m : & \quad \lambda_{max} = 1.8 + 0.9 * \frac{L_{crit} - 30}{50}
 \end{aligned}
 \tag{2.8}$$

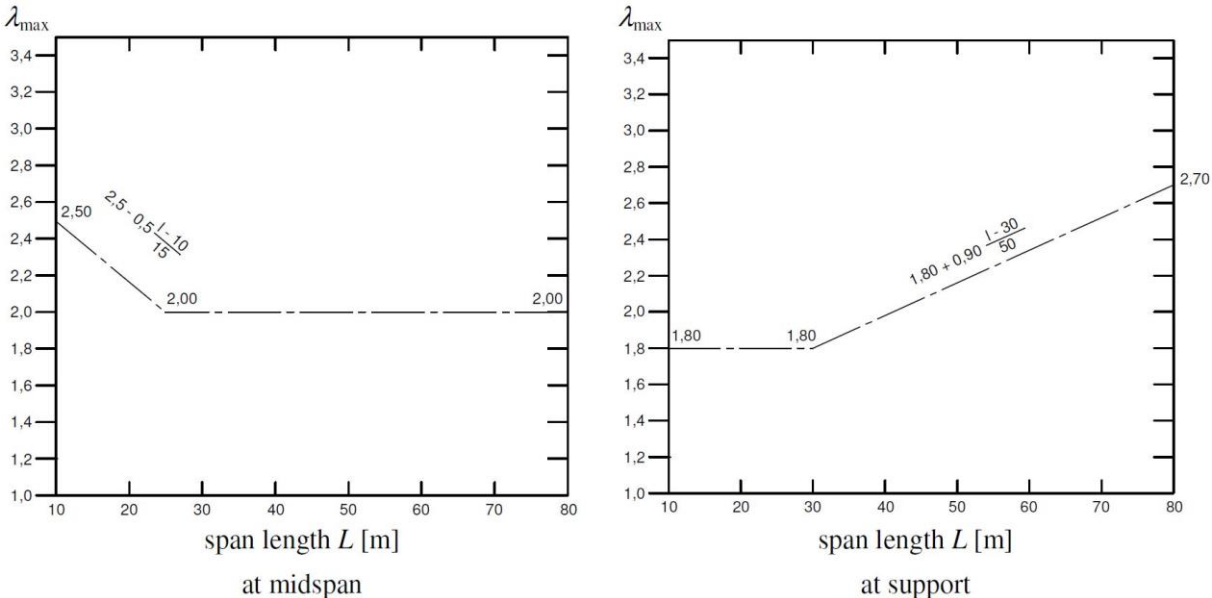


Figure 2.5 : λ_{max} for road bridge [8]

The first partial factor λ_1 represents the damage effect of traffic and depends on the critical length like λ_{max} . Its value should be determined as showed in the Figure 2.6:

- at midspan section:

$$\lambda_1 = 2.55 - 0.7 * \frac{L_{crit} - 10}{70} \quad (2.9)$$

- at support section:

$$\begin{aligned} L_{crit} < 30m : & \quad \lambda_{max} = 2.0 - 0.3 * \frac{L_{crit} - 10}{20} \\ L_{crit} \geq 30m : & \quad \lambda_{max} = 1.7 + 0.5 * \frac{L_{crit} - 30}{50} \end{aligned} \quad (2.10)$$

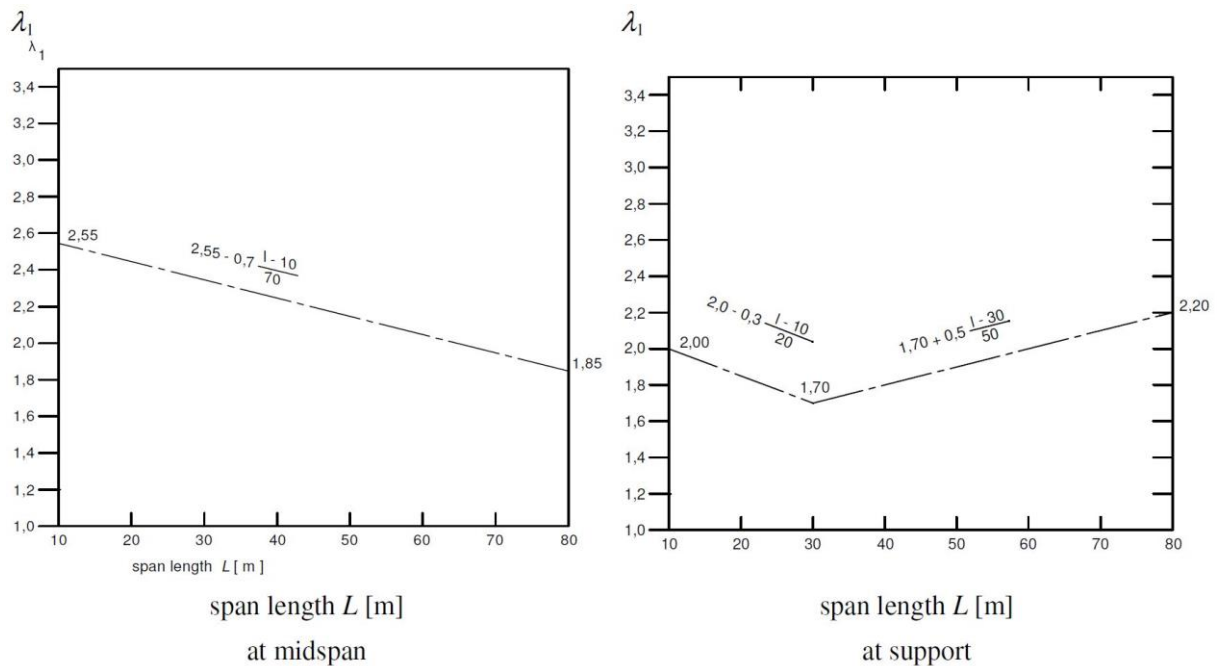


Figure 2.6 : λ_1 for road bridge [8]

λ_2 is the factor for the traffic volume and should be calculated as

$$\lambda_2 = \frac{Q_{m1}}{Q_0} \left(\frac{N_{obs}}{N_0} \right)^{1/5} = \frac{445}{480} \left(\frac{2 \cdot 10^6}{5 \cdot 10^5} \right)^{1/5} = 1.2233 \quad (2.11)$$

where Q_{m1} is the mean weight of the heavy traffic on the slow lane according to real traffic or, for example, to the FLM4 and then is equal to 445 kN, Q_0 is the reference value and is worth 480 kN, according to FLM3. N_{obs} and N_0 are equal respectively to 2×10^6 (table 4.5, EN 1991-2 [8]) and 0.5×10^6 (EN 1993-2 [7]) lorries per year. N_{obs} represents the number of heavy vehicles observed per year and per slow lane.

For different design working lives of the bridge, the partial factor λ_3 is used. It takes into account the design working life in years with the parameter t_{Ld} and should be calculated as follows:

$$\lambda_3 = \left(\frac{t_{Ld}}{100} \right)^{1/5} \quad (2.12)$$

In this project, a design lifetime of 100 years has been chosen and thus $\lambda_3 = 1.0$.

And finally, λ_4 represents the traffic on other lanes and considers particularly the number of heavy traffic per year (N_j) and the average weight of them (Q_{mj}). It should be calculated as follows:

$$\lambda_4 = \left[1 + \frac{N_2}{N_1} \left(\frac{\eta_2 Q_{m2}}{\eta_1 Q_{m1}} \right)^5 + \frac{N_3}{N_1} \left(\frac{\eta_3 Q_{m3}}{\eta_1 Q_{m1}} \right)^5 + \dots + \frac{N_k}{N_1} \left(\frac{\eta_k Q_{mk}}{\eta_1 Q_{m1}} \right)^5 \right]^{1/5} \quad (2.13)$$

However, the utilisation of the damage equivalent factor λ is limited. Indeed, on one hand it cannot be used for critical length higher than 80 meters, and on the other hand, if the influence line is complicated, it is not possible to find a comparison with simple influence lines and hence it is very difficult to determine correctly the critical length.

2.4. Damage accumulation

As a reminder, S-N curves have been determined with a constant stress range, but traffic load induces different $\Delta\sigma_i$. The influence of these various stress ranges can be taken into account with damage accumulation. Figure 2.7 shows a stress range histogram and its influence with one S-N curve.

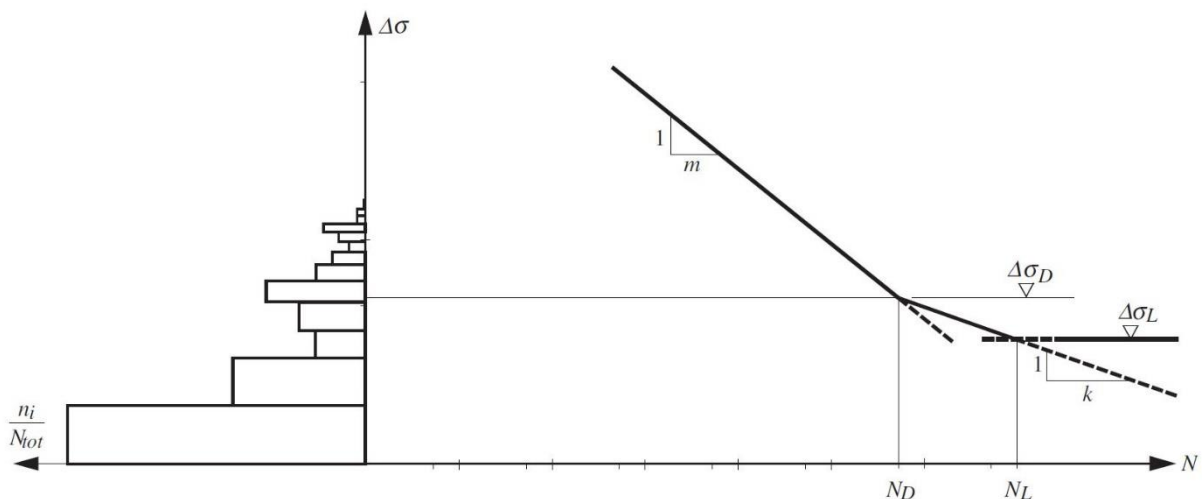


Figure 2.7 : Stress range histogram with S-N curve [2]

Each vehicle causes a partial damage to the structure with $\Delta\sigma_i$ being applied for n_i cycles and can be expressed as follows:

$$D_i = \frac{n_i}{N_{Ri}} \quad (2.14)$$

where N_{Ri} represents the number of cycles to failure under $\Delta\sigma_i$. It is possible to determine N_{Ri} with the relation (2.2), using CAFL at 5×10^6 cycles to calculate the constant C if the slope coefficient is 5 and using $\Delta\sigma_c$ at 2×10^6 cycles for a slope coefficient of 3. Thus, the partial damage should be calculated with the following expression, with m is equal to 3 or 5:

$$D_i = \frac{n_i}{N_{Ri}} = \frac{\Delta\sigma_i^m n_i}{CAF L^m \cdot 5 \cdot 10^6} \quad (2.15)$$

To obtain the total damage, each partial damage has to be summed and if the damage sum is equal to 1.0, the fatigue strength of the structure is reached. Hence, to ensure a good resistance, the next condition should be respected:

$$D_{tot} = \sum_i D_i \leq 1.0 \quad (2.16)$$

2.5. Fatigue load models

As a conclusion of this first chapter about the fatigue design, fatigue load models must be introduced. These models allow to define the traffic's characteristics that depend on the geometry of the vehicles, the axel loads, the vehicle spacing, the composition of the traffic and its dynamic effects (EN 1991-2) [9]. Five different fatigue models are defined for road bridges, denoted FLM1 to FLM5. In this project, only FLM3 to FLM5 will be presented because they are used to verify the fatigue lifetime's bridge, based on the S-N curves and fatigue assessment explained previously. Most of the information is pulled directly from the EN 1991-2 [9].

2.5.1. Fatigue load model 3

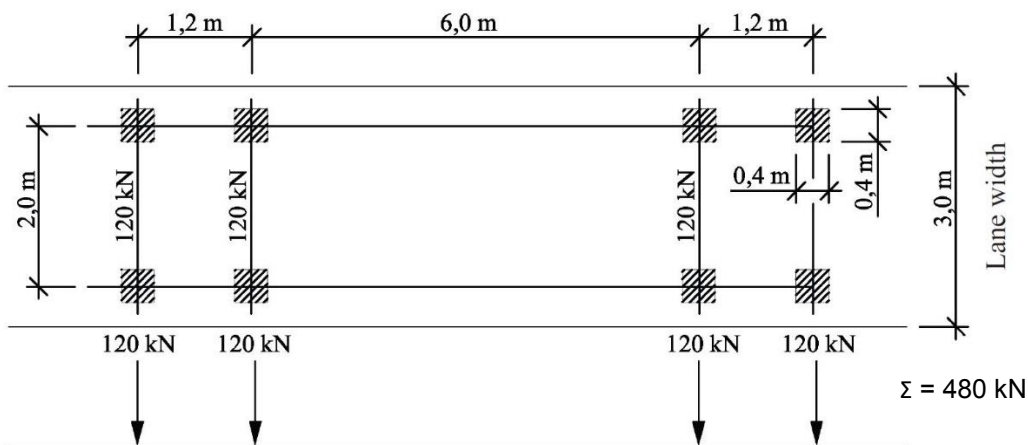


Figure 2.8 : Fatigue load model 3 [3]

Fatigue load model 3 is a simple model of a single vehicle with 4 axles of 120 kN each for a total weight of 480 kN and its geometry is shown in Figure 2.8. This model is very important for engineers because it is associated to the equivalent stress range at 2×10^6 cycles and the damage equivalent factor method. According to the EN 1991-2 [9], a second vehicle should be taken into account if it is relevant. The geometry of this second vehicle is the same as the first one with a reduced weight of 36 kN, instead of 120 kN, per axle and a minimum distance of 40 meters between the two vehicles.

2.5.2. Fatigue load model 4

Fatigue load model 4 is based on a set of five standard lorries as shown in Figure 2.9 that represent effects of a typical traffic on European roads. This model is associated to the damage accumulation and each lorry is taken into account alone with a certain percentage depending on the road type. In short, the five heavy vehicles total loads are:

$$Q_1 = 200 \text{ kN} \quad Q_2 = 310 \text{ kN} \quad Q_3 = 490 \text{ kN} \quad Q_4 = 390 \text{ kN} \quad Q_5 = 450 \text{ kN}$$

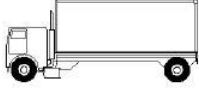
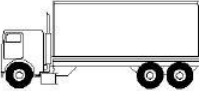
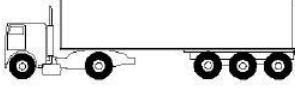


VEHICLE TYPE			TRAFFIC TYPE			
1	2	3	4	5	6	7
			Long distance	Medium distance	Local traffic	
LORRY	Axle spacing (m)	Equivalent axle loads (kN)	Lorry percentage	Lorry percentage	Lorry percentage	Wheel type
	4,5	70 130	20,0	40,0	80,0	A B
	4,20 1,30	70 120 120	5,0	10,0	5,0	A B B
	3,20 5,20 1,30 1,30	70 150 90 90 90	50,0	30,0	5,0	A B C C C
	3,40 6,00 1,80	70 140 90 90	15,0	15,0	5,0	A B B B
	4,80 3,60 4,40 1,30	70 130 90 80 80	10,0	5,0	5,0	A B C C C

Figure 2.9 : Fatigue load model 4 [9]

2.5.3. Fatigue load model 5

Fatigue load model 5 is the most general one and uses real traffic data based on statistics. A stress ranges histogram can be determined with counting methods, such as the reservoir or the rainflow, and thus, to verify the fatigue strength with damage accumulation.

3. Modelling of the study case

This chapter will present the study case on which this project is founded. This study case is based on the *Vasco da Gama* bridge and the main characteristics are taken from the PhD thesis of Professor José J. Oliveira Pedro [10].

The software used is the modelling software *SAP 2000* (SAP = Structural Analysis Program). It belongs to *Computers and Structures, Inc* (CSI), allows for structures modelling in 2D and 3D and for intern actions calculations. In this project, the entire work will be done with a 2D-model of half of the bridge. First, it will be presented the *Vasco da Gama* bridge, then the model used with the main differences with the *Vasco da Gama* bridge and the problems encountered.

3.1. Vasco da Gama bridge

The *Vasco da Gama* bridge is in Lisbon, the capital of Portugal. It is located in the eastern point of the city, crossing the Tagus River, and connects Lisbon to Setúbal. Its construction began in 1995 and the bridge was opened to the public in 1998. With a total length of 12.3 km, it is one of the longest bridges in Europe. It has also the characteristic to be made up of one cable-stayed part and viaducts parts. The first one interested us for this project.



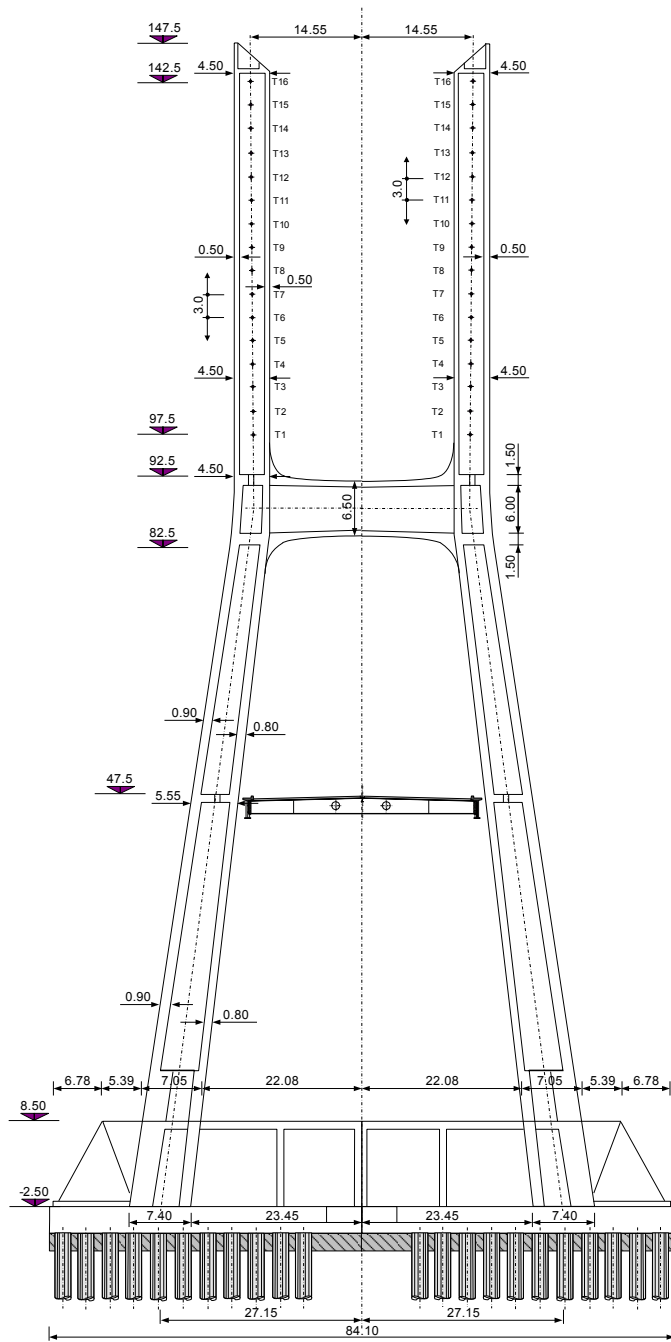
Figure 3.1 : Vasco da Gama bridge⁷

The bridge is entirely made of prestressed concrete. The cable-stayed part has a semi-harp shape and is composed by a central span of 420m and two lateral spans for a total length of around 830m. There

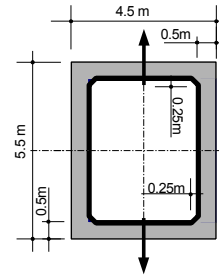
⁷ <http://tneurope.tableau-noir.net/pages13/images/pont-vasco-de-gama1.jpg>

are also two towers and six piers, three in each side span, which prevent excessive flexion in the towers. Finally, the whole is supported by four couples of 48 stays for a total of 192 stays.

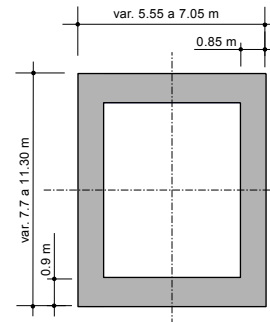
The towers have a H-shape and they are made of concrete. The height measures 150m and the width is 30m the top and 55m the base. The section is made of a concrete box with a steel box inside to absorb the traction transmitted by the stays. The top section equals 4.5m x 5.5m with a 0.5m thickness. The section is constant to link the stays then it varies linearly to the base and finally measures 7m x 11m with a 0.9m thickness. They are recessed in the ground and the deck is not fix to the tower. It is only retained by the stays, which they fix on the top of the towers as a semi-harp design.



Tower top section



Tower down section



Tapez une équation ici.

Figure 3.2 : Towers details [10]

Then, the deck has a width of 31m and allows three traffic-lanes if each direction. It is composed by two longitudinal girders made of prestressed concrete with a 2.6m x 1.7m section and transversal steel girders spaced 4.425m apart. The deck's geometry and its characteristics are showed in the Figure 3.3.

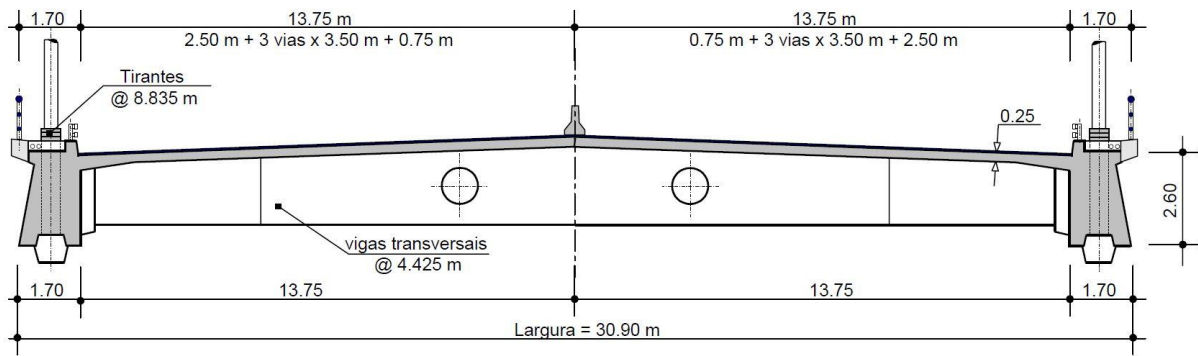


Figure 3.3 : Vasco da Gama deck [10]

Prestressed concrete longitudinal girders are used as support for the stays anchorage. The transversal girders allow a smaller thickness of the concrete and it equals to 0.25m.

3.2. SAP modeling

The main differences between the study case and Vasco da Gama bridge concern the deck and the number of stays. Indeed, as showed in the Figure 3.4, the study case deck is a composite steel-concrete one which is based on the PhD thesis of the Professor José J. Oliveira Pedro [10].

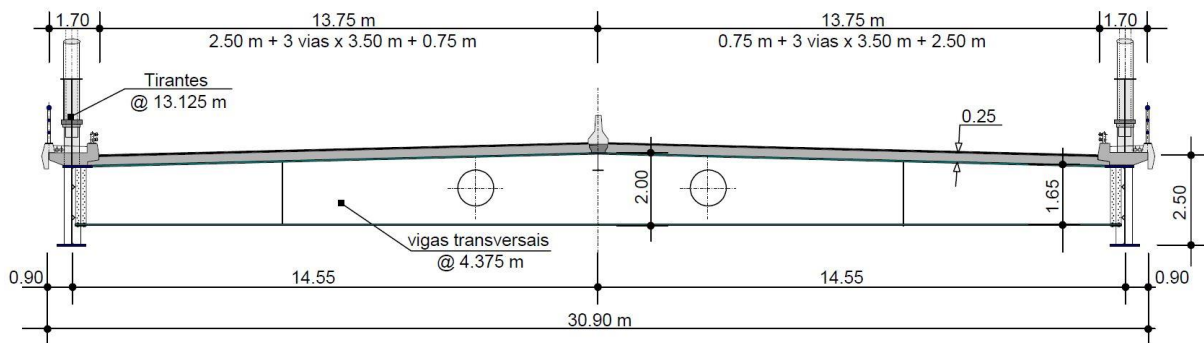


Figure 3.4 : Study case deck [10]

The longitudinal girders were replaced by I-shape steel girders with a height of 2.25m and longitudinal and transversal stiffeners. The transversal girders were kept but they are now spaced of 4.375m. The concrete part is composed by precast concrete slab panel with the same thickness of 0.25m. The connection between steel and concrete is insured with studs, as described in the Appendix 1. Moreover, the slab's reinforcement are ignored in this model and, as a 2D-model, it considers the half of the bridge's width with an effective concrete deck width of 7.5m ($b_{eff} = 7.5m$).

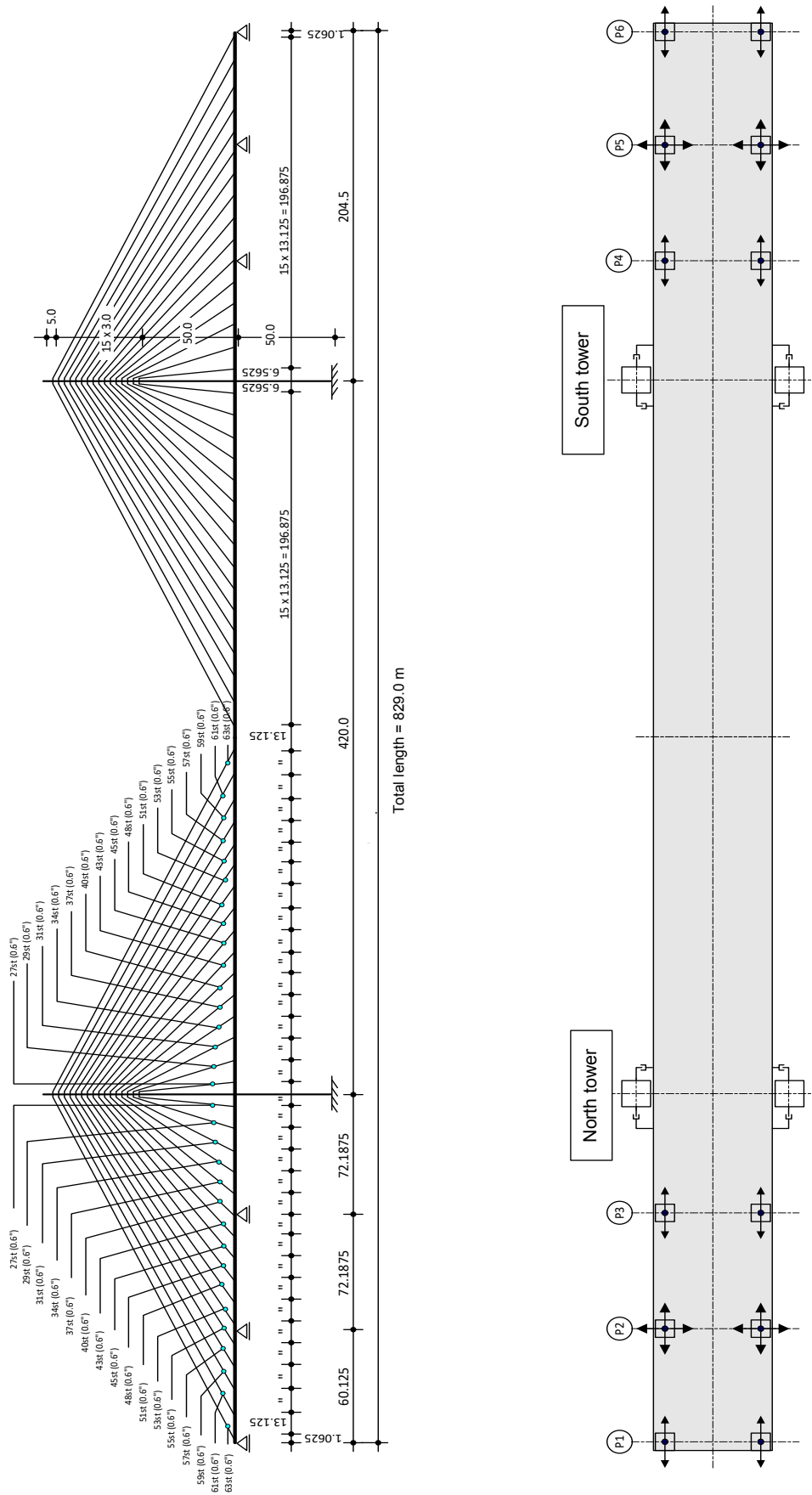


Figure 3.5 : Longitudinal configuration of the study case [10]

The longitudinal section of the study case is showed in the Figure 3.5. This model keeps the main dimensions of Vasco da Gama bridge, i.e. two lateral spans of 204.5m and a central span of 420m for a total of 829m in length. The towers and the piers are similar to the real Vasco da Gama bridge.

Regarding the stays, the study case is composed by four couples of 32 stays. However, as this project is done with a 2D-model, we consider only two couples of 36 stays for a total of 64 stays. These are directly linked to the main steel girders and are spaced with a distance of 13.125m (Appendix 1). For facilities, all the stays are numbered from L1 to L16 for lateral span and from C1 to C16 for central span, starting with the closest one to the tower. The dimensions vary between the first stay (near to the tower) with a diameter of 27 strands, which is equal to $27 * 150 \text{ mm}^2 = 4'050 \text{ mm}^2$, to the last stay with a diameter of 63 strands ($9'450 \text{ mm}^2$).

As this project want to perform fatigue verifications, it has been decided to model the deck with a concrete part (1) and a steel part (2), as described in the Figure 3.6. One also sees a stay connected to the steel (3). Then, to link concrete and steel, steel connectors (4) have been created.

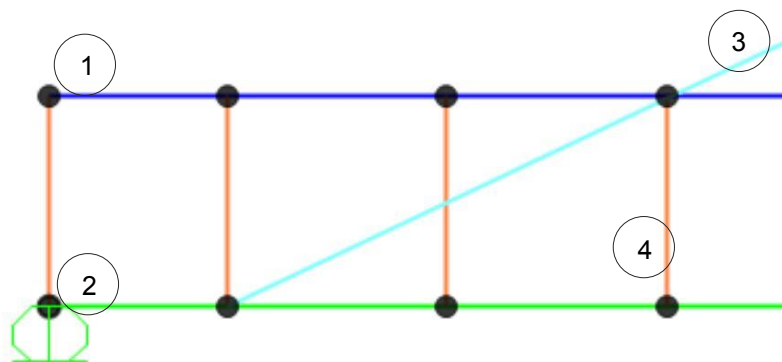


Figure 3.6 : Side view of the deck model

These connectors (4) are equivalent bars, to simulate 3 rows of stud steel connectors, made of steel with a diameter of 22mm. They are linked rigidly to the main girder (2) and the rotations are released in the concrete slab (1). The connectors have no mass and all connections have also been deleted between the deck and the towers.

Then, it appears one problem with the model. It's about linking the stays to the towers. Connectors have been also used to solve this problem. As there are only 16 stays (and no 24 as in the real Vasco da Gama bridge), they are spaced with a distance of 3m between each of them. They are linked to the deck on the steel part. There is no shearing, bending and torsional forces in the stays, so the frame releases are defined to permit only axial forces. The connectors created to link are steel rods too, but with a diameter of 1.5m. Indeed, they must maintain their physical shape and stay in the elastic range. These connectors are rigidly linked to the towers and replace the steel box used to absorb the stay's traction

in the Vasco da Gama bridge. The length of these connectors is the same that the width of the tower section in order to have the correct angle between each stay and the deck.

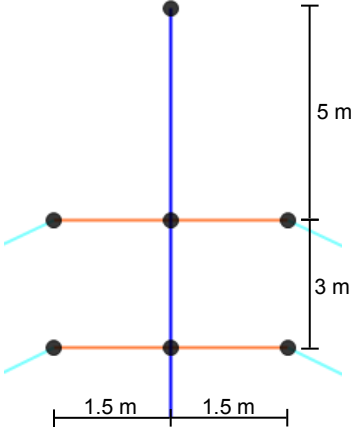


Figure 3.7 : Links between stays and towers

Finally, we have to define the different vertical loads which act on the bridge. Dead loads are composed of the weight of the supporting structure and the one of the equipment. It has been decided to consider the half of the value used in the PhD thesis of the Professor José J. Oliveira Pedro [10] to be coherent with modelling the half of the bridge, with an effective width of the precast concrete slab of 7.5m. Dead loads are detailed as follows:

- 100 kN/m for the precast concrete slab's weight
- 28 kN/m for the steel girders' weight
- 43 kN/m for the equipment

Thus, the total dead loads equal to: $g_{k,tot} = 171 \text{ kN/m}$

Traffic loads are defined by the different fatigue load model described in the first chapter.

3.2.1. Materials

About materials, these are the same as those used in the PhD thesis of the Professor José J. Oliveira Pedro [10]. The materials proprieties are presented in the **Erreur ! Source du renvoi introuvable.**

Table 1 : Materials details

Concrete			Steel			Stays		
Type	C 45/55	[-]	Type	S355 NL	[-]	Type	T15	[-]
$E_{c,0}$	44.17	[GPa]	E_s	44.17	[GPa]	Diam.	0.0152	[m]
γ_c	25	[kN/m ³]	γ_s	25	[kN/m ³]	Area	150	[mm ²]
$\sigma_{c,u}$	37.1	[MPa]	σ_s	37.1	[MPa]	E_e	195	:[GPa]
						σ_u	1770	[MPa]
						f_u	400	[MPa]

Deck connectors			Tower connectors		
Diam.	22	[mm]	Type	S355	[-]
f_u	400	[MPa]	Diam.	1500	[mm]

3.2.2. Stays tensioning

The last important point to talk about the 2D-model is the stays tensioning. Dead loads cause the first tension in the stays. But cable-stayed system only works if all the stays are in traction and never in compression because compression in one stay can cause damage to the bridge. Thus we have to pretension all the stays to avoid this problem but the difficulty is when one charges one stay, the tension in the other stays changes too. Based on the PhD thesis of the Professor José J. Oliveira Pedro [10], we have the desired installed forces F_{ha} and we want to recompute the required pretensions to obtain those F_{ha} .

Table 2 : Desired installed forces

	Stays	Forces [kN]	Stays	Forces [kN]
F_{ha}	16L	5816	1C	2203
	15L	5609	2C	2460
	14L	5240	3C	2592
	13L	5050	4C	2798
	12L	4835	5C	3096
	11L	4613	6C	3393
	10L	4365	7C	3579
	9L	4105	8C	3754
	8L	3826	9C	4121
	7L	3571	10C	4292
	6L	3264	11C	4677
	5L	3018	12C	4882
	4L	2841	13C	5114
	3L	2589	14C	5328
	2L	2446	15C	5501
	1L	2125	16C	5667

To obtain these forces, the following procedure must be followed:

- First step consists to apply dead load and obtain forces in each stay, which give us a 1x32 matrix called F_{cp}
- Then create 32 new loads cases for each pair of stays (L16 to L1 and C1 to C16) and apply a temperature's variation of $-1'000^{\circ}\text{C}$ ($\Delta T = -1'000^{\circ}\text{C}$). Build a 32x32 matrix, called M , with the previous results organized as columns.
- By importing SAP data files in Excel, evaluate the factor f to multiply the stay load cases, according to:

$$[M] \cdot f = F_{ha} - F_{cp} \quad (3.1)$$

$$f = [M^{-1}] \cdot \{F_{ha} - F_{cp}\} \quad (3.2)$$

- Create a load combination in SAP 2000 with f time each stay load case and dead load. This combination should produce at each stay the pretension forces initially announced F_{TIR} . It means that we must have:

$$F_{TIR} = F_{ha} \quad (3.3)$$

The obtained results are showed in the next table:

Table 3 : Calculated installed forces

	Stays	Forces [kN]	Stays	Forces [kN]
F_{TIR}	16L	5815.416	1C	2202.93
	15L	5609.417	2C	2460.468
	14L	5240.811	3C	2591.768
	13L	5049.821	4C	2797.918
	12L	4834.613	5C	3095.974
	11L	4613.171	6C	3392.622
	10L	4365.115	7C	3579.324
	9L	4105.393	8C	3754.491
	8L	3825.651	9C	4121.216
	7L	3570.456	10C	4291.22
	6L	3264.253	11C	4677.925
	5L	3017.74	12C	4881.475
	4L	2840.879	13C	5113.123
	3L	2589.429	14C	5327.976
	2L	2445.715	15C	5501.675
	1L	2124.867	16C	5667.285

By comparing the table 2 and the table 3, the forces are very similar, that means the relation (3.3) is satisfied. Moreover, in the Appendix 2, all the calculations and the matrix obtained are given.

4. Fatigue details

As explained in the first chapter, some details cause more fatigue problems than other, as connections (welds or studs) and geometrical changes. We must also choose which details we have to be studied and it is the aim of this chapter.

It is divided in two parts: the first one concern the main steel girder, which is subjected to bending and axial stresses and the second one is about the stays which are subjected to axial stresses only.

4.1. Selected details of bottom flange

In order to select a detail in the deck, it is possible to use the schema, described in the Figure 4.1, taken from SETRA guide (SETRA, 2010) [11], which is based on the Eurocodes. This figures shows different details of a composite deck with the associated FAT values.

Considering all the details we have in this project, it has been decided to choose the one which link the transversal stiffener with the bottom flange of the main girder. This detail, as showed in the Figure 4.1, has a FAT of 80 MPa because the width of the attachment is lower than 50mm.

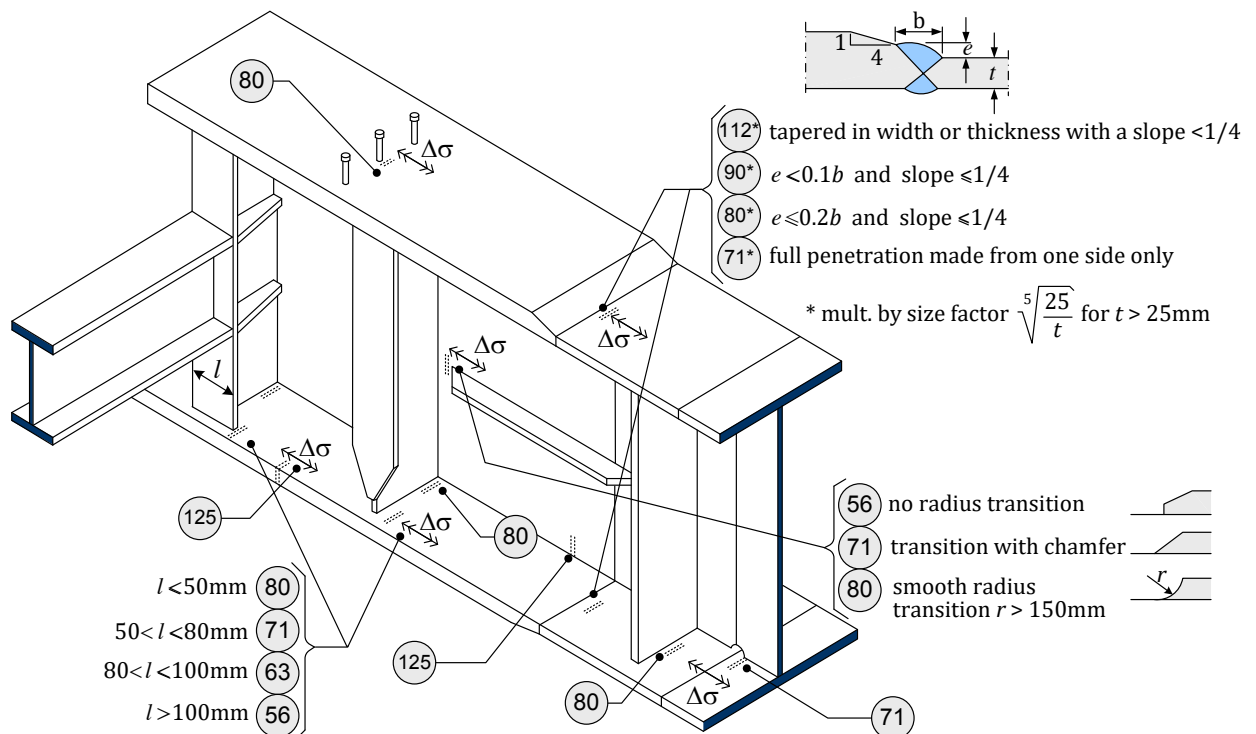


Figure 4.1 : Typical FAT detail categories (SETRA [11])

In order not to study every element of the bottom flange, we must select some particular elements which can represent the girder's behaviour. To do so, the curve of the envelop of the maximum and minimum stresses in the main girder is used. This curve is based on four parameters: the maximal bending moment, the minimal bending moment, the maximum axial force and the minimum axial force in the steel part. The stresses are calculated with the internal forces using the following relation, with N positive defined as tension:

$$\Delta\sigma_B = \frac{\Delta M}{W} + \frac{\Delta N}{A} = \frac{M_{max,t1} - M_{min,t2}}{W} - \frac{N_{max,t1} - N_{min,t2}}{A} \tag{4.1}$$

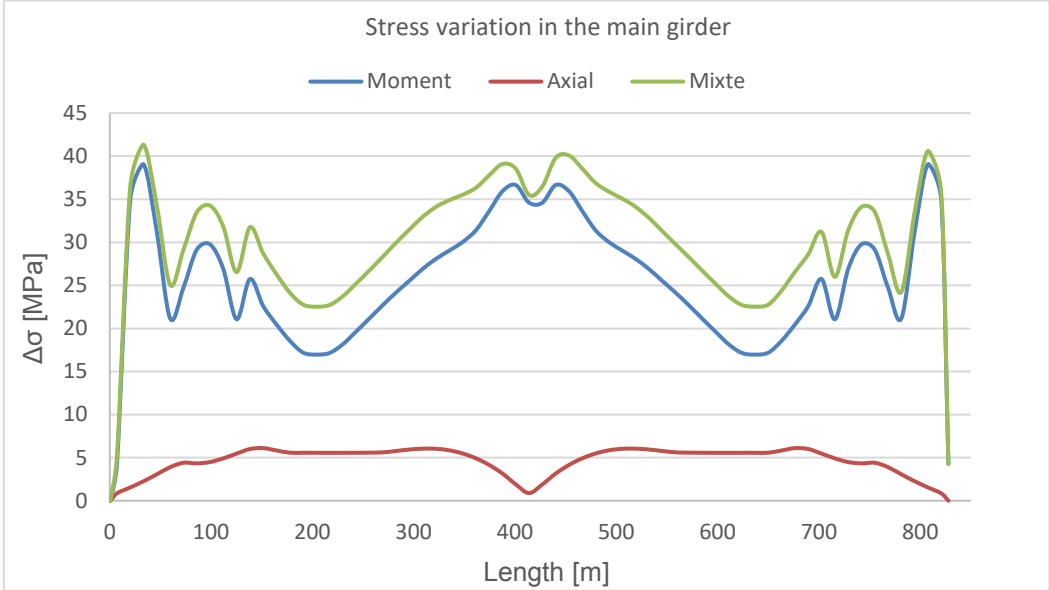


Figure 4.2 : Stress variation in the main girder due to FLM3

As we can see in the Figure 4.2, the axial stress has a little impact on the total one and the bending stress is very similar to the total stress of the main girder (70 to 90%). In this fact, it has been decided to use the maximal variation of the bending stresses to determine the total stress in the bottom flange and add the associated normal stresses, even if it is not the maximum and minimum. Still based on the Figure 4.2, it is possible to select five elements to perform fatigue verification procedures. These elements are showed in the Figure 4.3.

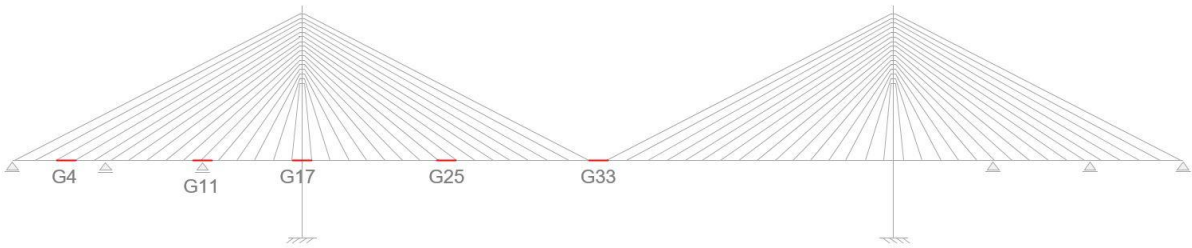


Figure 4.3 : Selected elements of the main girder

As the bridge is symmetrical, the selected elements are located only in the first half of the bridge and are:

- G4 which represents the maximum $\Delta\sigma$ and is at 33m of the most left point of the bridge
- G11 which is on the second pier at 125m
- G17 which represents the minimum $\Delta\sigma$ and is located around the first tower at 204m
- G25 which represents the average stress variation and is at 309m
- G33 which represents the element in the middle of the central span at 415m

One last important point to mention concern the relation (4.1). Indeed, the section area equals to $A = 0.1464 \text{ m}^2$ and represents the area of the main steel girder's section. The section modulus value W is calculated in such way to obtain the stress at the weld between the stiffener and the bottom flange. This parameter should be determined as follows, with an inertia equals to $I = 0.14 \text{ m}^4$:

$$W = \frac{I}{\frac{h}{2} - \frac{t_{inf}}{2}} \tag{4.2}$$

4.2. Selected details of stays

Regarding the details of stays, we must first analyse their anchorage. The Figure 4.4 shows us what is the anchor type, directly welded to the main steel girder. This anchorage is composed by a steel sheet with two stiffeners. The stay is then put in the available space and fixed with a ring.

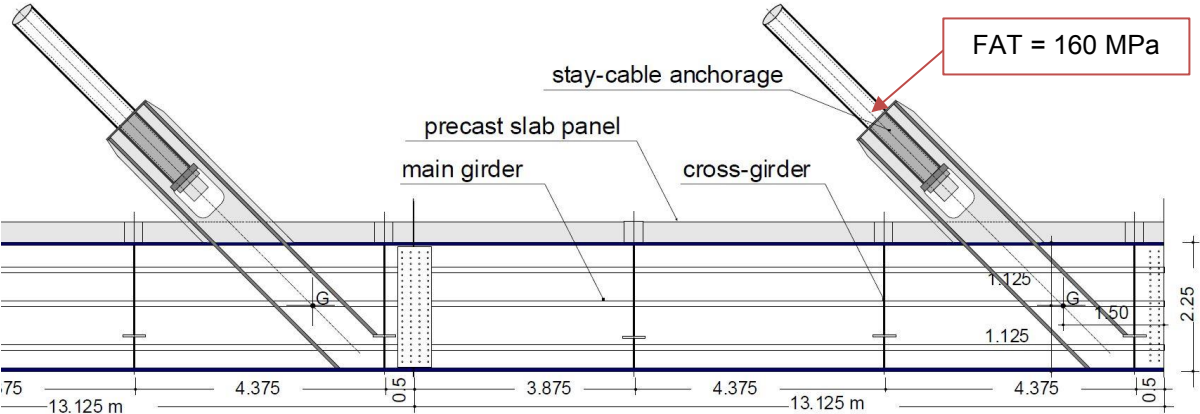


Figure 4.4 : Details of the anchorage of the stays

So, there are a lot of details but in order to seek simplicity, the selected detail is the stay's breaking close to the anchorage. This detail allows us to use some simplifications for the next calculations such as to only have axial forces in the stay. According to the EN 1993-1-11 [6], this detail has a FAT value of 160 MPa from the fact that the stays are made of strands.

Group	Tension components		Detail category $\Delta\sigma_c$ [N/mm²]
A	1	Prestressing bars	105
B	2	Fully locked coil rope with metal or resin socketing	150
	3	Spiral strands with metal or resin socketing	150
C	4	Parallel wire strands with epoxy socketing	160
	5	Bundle of parallel strands	160
	6	Bundle of parallel wires	160

Figure 4.5 : Table 9.1 of EN 1993-1-11 [6]

5. Influence lines

This chapter present one of the most important points of this project: influence lines. Indeed, the influence line allows to define the stress range in one element in a specific location under mobile load. Using a unitary mobile load, we just have to multiply the influence line's curve by the value of the total load of the vehicle to obtain the wanted stress ranges. Thus, using influence line is a great advantage.

There are two types of influence lines: the ones which are based on forces and the ones which are based on stresses. Those using forces are the most common but in this project, it is better to use the ones with stresses. Indeed, in the case of cable-stayed bridge, the deck is subjected to bending forces and axial forces which are introduced by stays. In order to take it into account, we have to use the relation (4.1) as described in the previous chapter.

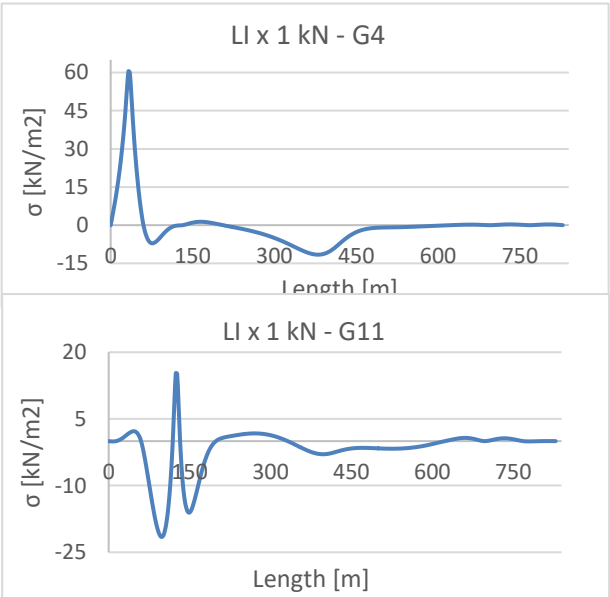
Moreover, with influence lines, it is possible to define the critical length which are important in the damage equivalent factor procedure (§2.3), This length is calculated according to the influence line's type. Using the EN 1993-2 (article 9.5.2) [8], the critical length may be defined for simple influence lines. In the Appendix 3 ,there are the main influence lines used in this project to define critical lengths of the stress influence lines obtained.

5.1. Stress influence lines of bottom flange

For elements of bottom flange defined in the previous chapter, the influence lines are presented below:

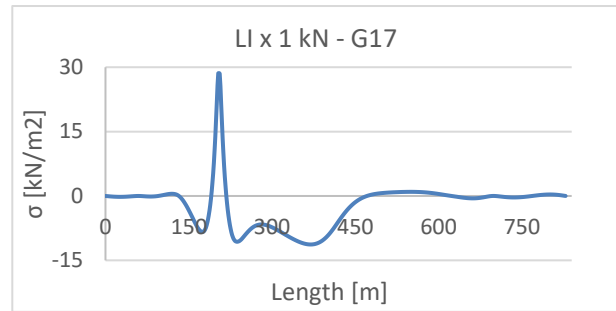
- *Element G4:*
Similar to a bending force in midspan section
 $L_{crit} = L_i = 61 \text{ m}$

- *Element G11:*
Similar to a bending force in midspan section
 $L_{crit} = L_i = 15 \text{ m}$



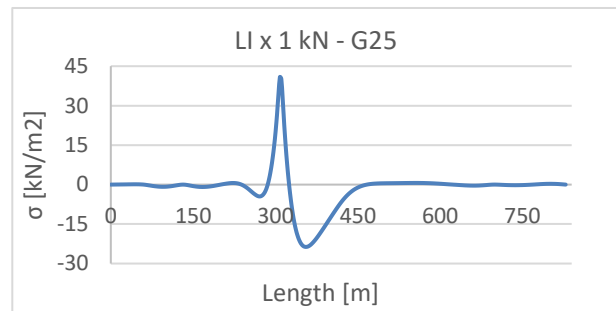
- **Element G17:**
Similar to a bending force in midspan section

$$L_{crit} = L_i = 30 \text{ m}$$



- **Element G25:**
Similar to a shear force in midspan section

$$L_{crit} = 0.4 \times L_i = 70 \text{ m}$$



- **Element G33:**
Similar to a bending force in midspan section

$$L_{crit} = L_i = 65 \text{ m}$$

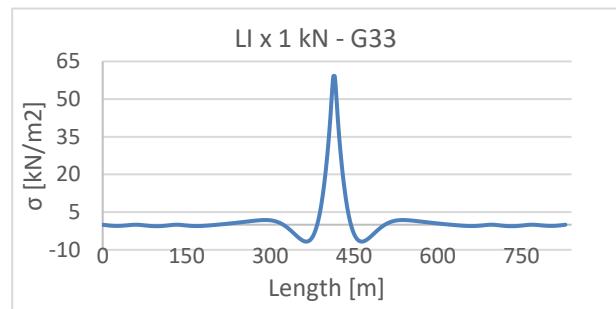


Figure 5.1 : Influence lines of bottom flange elements

We first notice that these influence lines are not complicated. This allows to compare them easily with the ones of the Appendix 3. Then, critical lengths are all lower than the Eurocode limit, which is 80m. In the next steps, this will allow to perform the different fatigue verification procedures with well-known data. In the table below, all the information about influence lines of the bottom flange's elements are summarized:

Table 4 : Critical length for elements of the bottom flange

N°	Equivalent to	L_{crit}
G4	Moment - Midspan	60
G11	Moment - Midspan	15
G17	Moment - Midspan	30
G25	Shear - Midspan	70
G33	Moment - Midspan	65

5.2. Stress influence lines of stays

There are two types of stays: the central one and the lateral ones. And these give two types of influence lines. As showed in Figure 5.2, lateral stays are irregular with complex influence lines. It involves that the critical lengths are difficult to determine. The Appendix 4 presents a summarize of each influence line of lateral stays with the critical length associated.

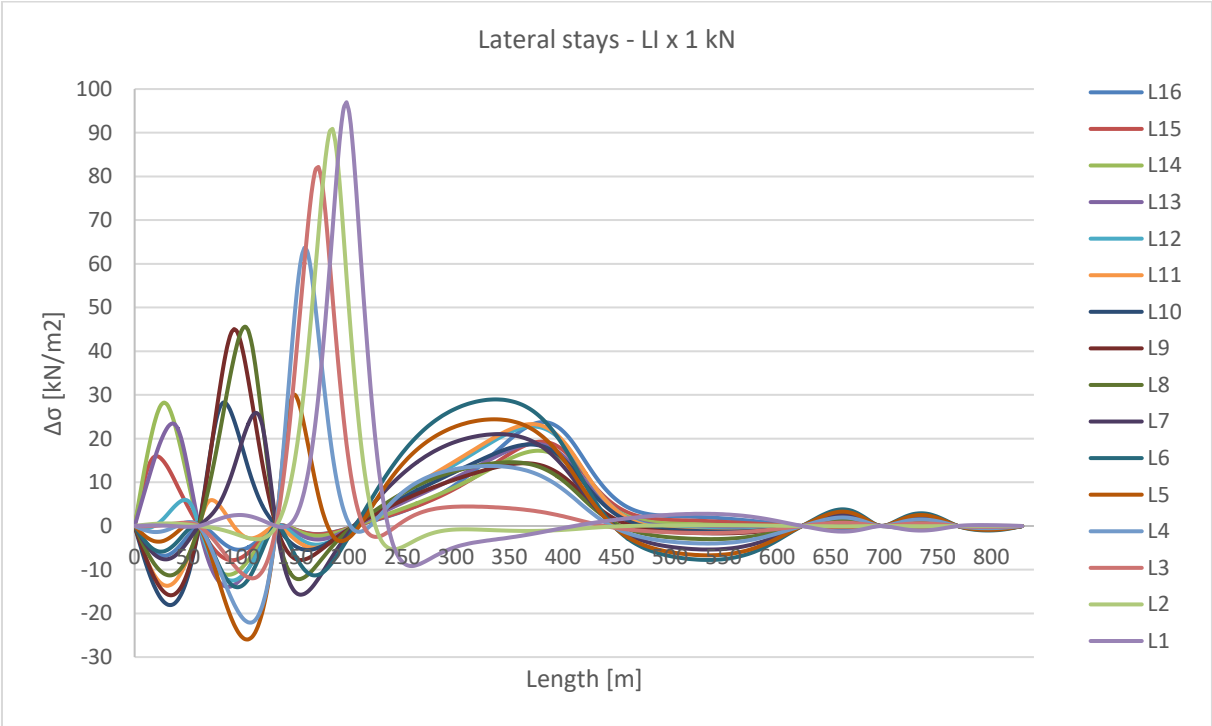


Figure 5.2 : Influence lines of lateral stays

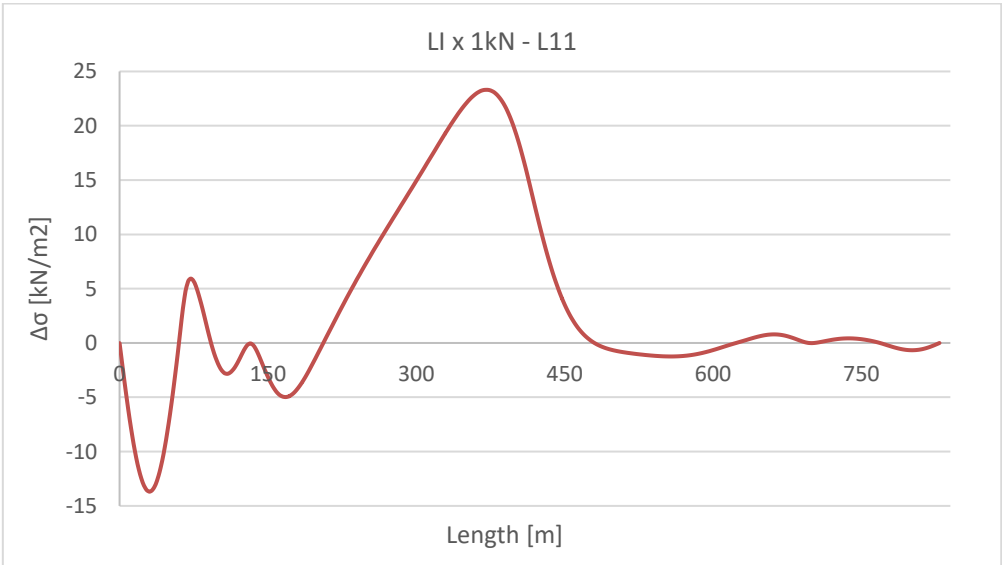


Figure 5.3 : Influence line of L11

One has really been difficult to determine and it is the lateral stay 11 (*L11*). This one represents the stay link to the second pier (*P2*). With his complex shape, it hasn't been possible to compare it with a simple influence line. It has been decided to take a support section with a critical length equal to 100m because it is the most unfavourable value.

For the central stays, it is more simple. Indeed, they are regular with a simple shape. We can compare them to the influence line of a moment in a midspan section. So the critical length is the length between the points that cross the abscise. However, for the *C15* and *C16*, they are more similar to the influence line of a shear force in a midspan section.

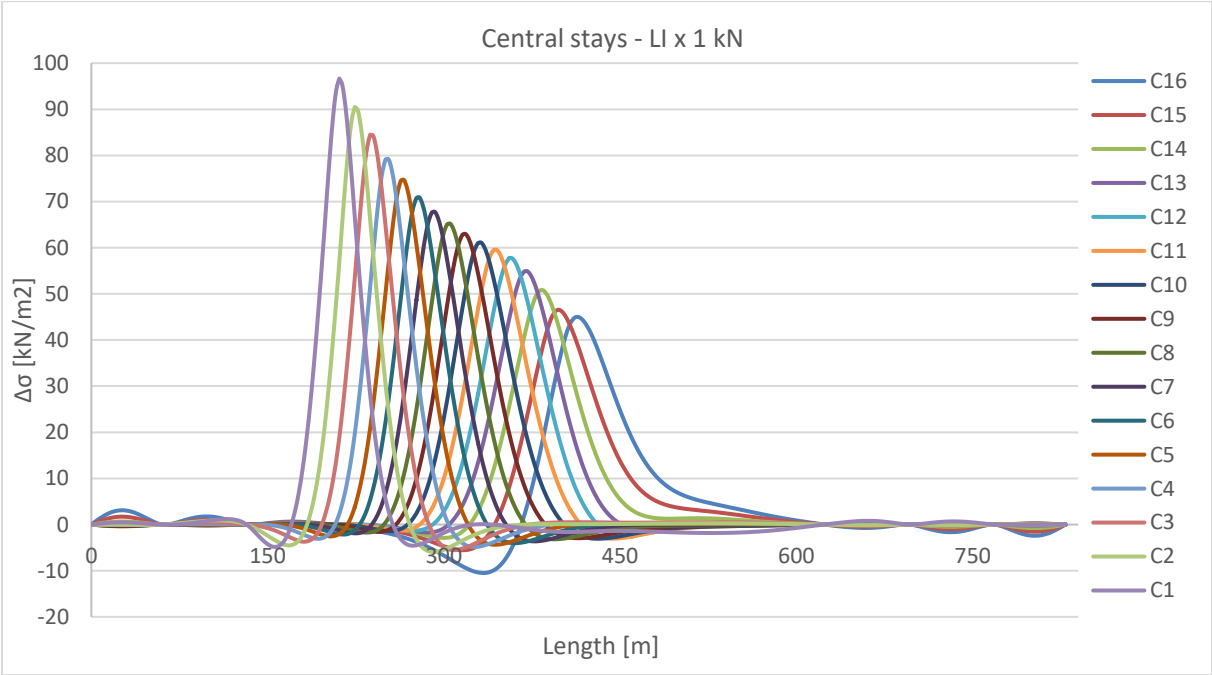


Figure 5.4 : Influence lines of central stays

In the **Erreur ! Source du renvoi introuvable.**, critical lengths obtained for stays are summarized:

Table 5 : Critical lengths for stays

N°	Force - Section	L _{crit} [m]	N°	Force - Section	L _{crit} [m]
L1	Moment - Midspan	89	C1	Moment - Midspan	89
L2	Moment - Midspan	100	C2	Moment - Midspan	90
L3	Moment - Midspan	81	C3	Moment - Midspan	90
L4	Moment - Support	315	C4	Moment - Midspan	90
L5	Moment - Support	315	C5	Moment - Midspan	105
L6	Moment - Support	145	C6	Moment - Midspan	100
L7	Moment - Midspan	71	C7	Moment - Midspan	100
L8	Moment - Midspan	71	C8	Moment - Midspan	100
L9	Moment - Midspan	71	C9	Moment - Midspan	125
L10	Moment - Midspan	71	C10	Moment - Midspan	130
L11	Support	100	C11	Moment - Midspan	145
L12	Moment - Support	140	C12	Moment - Midspan	150
L13	Shear - Midspan	54	C13	Moment - Midspan	150
L14	Shear - Midspan	54	C14	Moment - Midspan	160
L15	Shear - Midspan	54	C15	Shear - Midspan	162
L16	Moment - Support	135	C16	Shear - Midspan	162

As one can notice, influence lines are much higher than the Eurocode limit of 80m. In this fact, hypotheses should be done in order to determine partial factors with the critical length. These hypotheses are based on the researches and results of the PhD thesis of Nariman Maddah (Maddah, 2013) [5] and are presented in the chapter on fatigue verification procedures for stays.

6. Fatigue assessment of bottom flange

The objective of this chapter is to explain the different fatigue verification procedures. Indeed, before perform the verifications with the stay which have critical lengths higher than the Eurocode limit, it is better to apply these procedures to elements with well-known data. The following procedures are based on two models: *Fatigue load model 3* (FLM3 - §2.5.1) and *Fatigue load model 4* (FLM4 - §2.5.2).

With FLM3, the damage equivalent factor λ is used and allows to compare the FAT value with the equivalent stress range at 2×10^6 cycles. With FLM4, damages are determined for each lorry which composes the model (Figure 2.9) and we have to verify that the total damages stay below than 1.0.

Moreover, in order to explain the procedures with more details, all calculations are based on the element G4 of the main girder. As reminder, this element represents the maximal stress variation for the bottom flange. Calculations and formulas are mainly based on the standard rules described in the Eurocodes.

6.1. Verification using the damage equivalent factor

As previously explained and using the theory described in the first chapter, the damage equivalent factor allows to determine the equivalent stress range at 2×10^6 cycles and to compare it with the FAT value, which represents the value of the S-N curve for 2×10^6 cycles. It is then possible to re-write the relation (2.4) in order to compare directly the FAT value, by taking into account of the safety factors:

$$\gamma_{Mf} \cdot \gamma_{Ff} \cdot \Delta\sigma_{E2} \leq \Delta\sigma_C \quad (6.1)$$

Moreover, to determine the stress range in the bottom flange, a load of 480 kN is used (FLM3), which moves all along the influence line of the selected element (here G4). The multiplication of this load with the values of the unitary influence line give us all the stresses in the bottom flange. We have to find the maximal and minimal one to determine the maximum stress range. It is also assumed as hypothesis that only one heavy vehicle moves on only traffic lane, which allows to simplify some parameters.

Based on the relation (2.3) and the next ones, the different partial factors can be calculated. With a working life of 100 years and only one lane for heavy vehicles, partial factors λ_3 and λ_4 equal to 1.0. Then, as the Eurocodes are based on a heavy traffic of 5×10^5 HV (heavy vehicle)/year/lane, we have to use λ_2 to be able to calculate for a heavy traffic of 2×10^6 HV/year/lane.

In the following table, calculations are summarized:

Table 6 : Fatigue verification with FLM3 for element G4

		LI x 480 kN
Force		Bending
Section		Midspan
L_{crit}	[m]	61
λ_1	[-]	2.04
Q_0	[kN]	480
N_0	[-]	5.00E+05
Q_{m1}	[kN]	445
N_{obs}	[-]	2.00E+06
λ_2	[-]	1.22
λ_3	[-]	1.00
λ_4	[-]	1.00
λ	[-]	2.50
λ_{max}	[-]	2.00
$\Delta\sigma_B$	[MPa]	34.60
λ	[-]	2.00
$\Delta\sigma(Q_{fat})$	[MPa]	34.60
$\Delta\sigma_{E,2} \times 1.35$	[MPa]	93.42
$\Delta\sigma_C$	[MPa]	80.00
Verification		NOT OK

First, the verification is not satisfied with a safety factor of 1.35 (93.42 MPa > 80.00 MPa). To fix it one solution could be to reinforce the bottom flange, which allows to reduce the stresses at this particular place. Then, one observes that the λ factor is higher than λ_{max} , so this last one is used to determine the equivalent stress range.

By varying the selected elements and the associated influence lined, we apply this verification to the other elements and the obtained results are showed in the following table:

Table 7 : Fatigue verification with FLM3 for the bottom flange

		G4	G11	G17	G25	G33
Force		Bending	Bending	Bending	Shear	Bending
Section		Midspan	Midspan	Midspan	Midspan	Midspan
L_{crit}	[m]	61	15	30	70	65
λ	[-]	2.50	3.06	2.87	2.39	2.45
λ_{max}	[-]	2.00	2.33	2.00	2.00	2.00
$\Delta\sigma_{E,2} \times 1.35$	[MPa]	93.42	55.69	51.65	83.66	85.21
$\Delta\sigma_C$	[MPa]	80.00	80.00	80.00	80.00	80.00
Verification		NOT OK	OK	OK	NOT OK	NOT OK

Only two elements are satisfied with the fatigue resistance. So the solution of a reinforcement in some locations of the main girder could be a good solution to reduce the stresses. However, the λ factor is higher than the λ_{max} for all the elements. This involves that we use a lower λ factor than the one is calculated.

6.2. Verification using the damage accumulation method

In regards to the procedure with FLM4, we must calculate damages caused by each lorry individually and then verify that the total is lower than 1.0 according to the relation (2.16). As the previous procedure, only one vehicle is considered on the influence line. Based on the Figure 2.9, we have to take into account a percentage for each lorry according to the traffic type. In this project, it is considered *long distance*.

Then, damage is based on the fatigue curve of the selected detail. In this case, we have a FAT value of 80 MPa and slope's coefficient of 3 and 5 according to the stress range. Moreover, a cut-off limit should be considered and involves that stress ranges lower than this limit cause no damage. Based on the Figure 2.2, the important values are:

$$\Delta\sigma_C = FAT = 80 \text{ MPa} \quad (6.2)$$

$$\Delta\sigma_D = CAFL = 0.74 \cdot \Delta\sigma_C = 58.96 \text{ MPa} \quad (6.3)$$

$$\Delta\sigma_L = \text{Cut-off limit} = 0.405 \cdot \Delta\sigma_C = 32.37 \text{ MPa} \quad (6.4)$$

Table 8 : Fatigue verification with FLM4 for element G4

		G4					
		Q1	Q2	Q3	Q4	Q5	
$\Delta\sigma_C$	[MPa]	80	80	80	80	80	
$\Delta\sigma_D$	[MPa]	58.96	58.96	58.96	58.96	58.96	
$\Delta\sigma_L$	[MPa]	32.37	32.37	32.37	32.37	32.37	
Distribution	[%]	20%	5%	50%	15%	10%	
n_i	[veh]	4.00E+07	1.00E+07	1.00E+08	3.00E+07	2.00E+07	
$\Delta\sigma_B$	[MPa]	19.46	30.17	47.69	37.95	43.79	
m	[-]	0	0	5	5	5	
C_3	[-]	1.02E+12	1.02E+12	1.02E+12	1.02E+12	1.02E+12	
C_5	[-]	3.56E+15	3.56E+15	3.56E+15	3.56E+15	3.56E+15	
n_i	[veh]	4.00E+07	1.00E+07	1.00E+08	3.00E+07	2.00E+07	
N_{Ri}	[-]	Nothing	Nothing	1.44E+07	4.52E+07	2.21E+07	
D_i	[-]	0	0	6.9211	0.6632	0.9043	
Verification							8.4886

To calculate the resistant number of cycle N_{Ri} , we have to calculate the constant of the S-N curve for a slope's coefficient of 3 and 5. To do so, the relation (2.2) is used, knowing that the CAFL at 5×10^6 cycles is common to both slopes. One will notice that the vehicle 3 with a load of 490 kN causes more than 80% of the total damages alone. That can be explained as this vehicle represents 50% of the heavy traffic. Finally, total damages equal to 8.5 which clearly more than 1.0. Thus, fatigue with FLM4 is not satisfied.

To confirm or not, this procedure is applied to the other elements of the bottom flange and the obtained results are showed in the following table:

Table 9 : Fatigue verification with FLM4 for the bottom flange

		G4	G11	G17	G25	G33
$\Delta\sigma_D$	[MPa]	58.96	58.96	58.96	58.96	58.96
$\Delta\sigma_L$	[MPa]	32.37	32.37	32.37	32.37	32.37
$\Delta\sigma_B$ (veh.3)	[MPa]	47.69	24.36	26.37	42.70	43.49
D_{tot}	[-]	8.49	0.00	0.00	4.89	5.36

Trends are similar for the other elements of the bottom flange. The vehicle 3 still represents more than 80% of total damages when damages occur. The conclusion is that it is possible to use only the vehicle 3 for damage accumulation. It would be another *Fatigue load model 3*.

Moreover, results are similar with those calculated with damage equivalent factor procedure. However, it would be interesting to compare damages with the both procedures.

6.3. Conclusions

First of all, damages obtained with damage equivalent factor verification must be calculated. To do so, we have to divided the equivalent stress range at 2×10^6 cycles with the FAT value and take into account the slope coefficient m , as described in the next relation:

$$D_{tot} = \left(\frac{\Delta\sigma_{E,2}}{FAT} \right)^m \quad (6.5)$$

Table 10 presents a summary according to the procedure used:

Table 10 : Comparison damages for the bottom flange

			G4	G11	G17	G25	G33
FLM3	λ	[-]	2.5	3.06	2.87	2.39	2.45
	D_{tot}	[-]	2.19	0.17	0.12	1.28	1.40
FLM4	D_{tot}	[-]	8.49	0	0	4.89	5.36

The first observation is that damages cannot be compared, because the two fatigue load model are not similar. Indeed, the number of cycle of each model is different. FLM3 is based on 2 million of cycles when FLM4 is based on 100 million of cycles. In brief, we can write it as follows:

FLM3	–	$Q = \lambda \times 480 \text{ kN}$	–	$N = 2 \times 10^6 \text{ cycles}$
FLM4	–	$Q = 490 \text{ kN}$	–	$N = 100 \times 1 \times 10^6 \text{ cycles}$

We can also precise that FLM4 is used to determine local effects for short spans ($L \approx 10\text{m}$) when FLM3 is used for lengths until 80m.

7. Fatigue assessment of stays

The objective of this chapter is comparable to the previous but this time it is for stays. The main differences are that the selected detail for stays is subjected only to an axial effort and that the critical lengths are higher than the Eurocode limit of 80m. In this fact, hypotheses should be done on the λ factor value for critical length higher than 80m in order to verify stays with damage equivalent factor procedure.

To do so, hypotheses are based on the PhD thesis of Nariman Maddah [5] and the results he obtained. These results are based on the Swiss traffic with $N_0 = 500'000$ heavy vehicles per year using FLM4 with traffic type of *long distance* and are showed in the Figure 7.1.

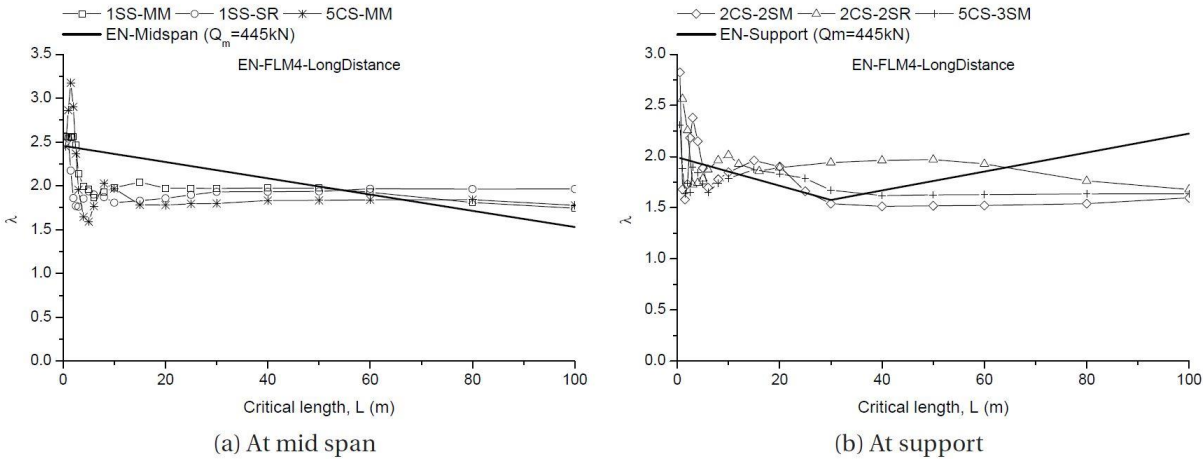


Figure 7.1 : Comparison of Eurocode damage equivalent factor with FLM4 for long distance traffic

One observes that the trend for critical length between 80m and 100m is constant for a midspan section or a section at support. It has been then decided to keep the value of the partial factor λ_1 in this thesis constant for critical lengths higher than 80m, written as follows:

$$\begin{array}{llll}
 \lambda_1 & \rightarrow & = 1.85 \text{ (midspan)} & \& = 2.20 \text{ (support)} \\
 \lambda_{max} & \rightarrow & = 2.00 \text{ (midspan)} & \& = 2.70 \text{ (support)}
 \end{array}$$

Then only 5 stays will be presented and they are the ones with maximal and minimal stresses in the lateral and central spans ($L1, L16, C1$ and $C16$) and also $L11$ because its influence line is very complex. All calculations for each 32 stays are in the Appendix 5. Calculations and formulas are mainly based on the standard rules described in the Eurocodes.

7.1. Verification using the damage equivalent factor

Based on the same methodology as described in the previous chapter (§6.1), the values of the next partial factors are identical:

$$\lambda_2 = 1.22$$

$$\lambda_3 = 1.00$$

$$\lambda_4 = 1.00$$

The partial factors λ_1 and λ_{max} are based on the hypotheses made for critical lengths higher than 80m. The obtained results are presented in the following table:

Table 11 : Fatigue verification with FLM3 for the stays

		L16	L11	L1	C1	C16
Force		Bending	-	Bending	Bending	Shear
Section		Support	Support	Midspan	Midspan	Midspan
L_{crit}	[m]	135	100	100	90	162
λ	[-]	2.69	2.69	2.26	2.26	2.26
λ_{max}	[-]	2.70	2.70	2.00	2.00	2.00
$\Delta\sigma_{E,2} \times 1.35$	[MPa]	53.38	64.52	137.57	131.55	71.93
$\Delta\sigma_C$	[MPa]	160.00	160.00	160.00	160.00	160.00
Verification		OK	OK	OK	OK	OK

One will first notice that all critical lengths are higher than 80m. That involves that the values of λ factor vary between 2.26 for midspan section and 2.69 for section at support. These values are close or higher to the maximal limit according to the Eurocode (λ_{max}). As reminder, influence line of the stay *L11* is complex and thus, it has been decided to take a critical length of 100m for a section at support because it is the most unfavourable value for λ factor.

Then, all the stays satisfy the fatigue verification. However, this is not enough to confirm that the constant trend hypotheses are corrects.

7.2. Verification using the damage accumulation method

The procedure based on FLM4 is now performed. All matters relating to the traffic is similar to the procedure for the bottom flange elements. However, damage accumulation is based on the S-N curve for tension components (Figure 2.3). The main differences are that the slope's coefficients equal 4 and 6 and that there is no cut-off limit, which involves that all stress ranges cause damages.

The details of the damage accumulation for the stay L1 is described in the following table:

Table 12 : Fatigue verification with FLM4 for stay L1

		L1					
		Q ₁	Q ₂	Q ₃	Q ₄	Q ₅	
$\Delta\sigma_C$	[MPa]	160.00	160.00	160.00	160.00	160.00	
Distribution	[%]	20%	5%	50%	15%	10%	
n_i	[veh/an]	4.00E+07	1.00E+07	1.00E+08	3.00E+07	2.00E+07	
$\Delta\sigma_N$	[MPa]	28.66	44.42	70.22	55.89	64.49	
m	[-]	6	6	6	6	6	
n_i	[veh/an]	4.00E+07	1.00E+07	1.00E+08	3.00E+07	2.00E+07	
N_{Ri}	[-]	6.05E+10	4.37E+09	2.80E+08	1.10E+09	4.67E+08	
D_i	[-]	0.0007	0.0023	0.3571	0.0273	0.0428	
Verification							0.4302

As for the verification of the bottom flange element, damages caused by the vehicle 3 represent more than 80% of the total damages. Moreover, damages are clearly lower than 1.0 and so fatigue verification is satisfied. However, this damages value is very low and not common. These results can be compared with the other stays, as follows:

Table 13 : Fatigue verification with FLM4 for the stays

		L16	L11	L1	C1	C16
$\Delta\sigma_C$	[MPa]	160	160	160	160	160
$\Delta\sigma_N$ (veh.3)	[MPa]	20.25	24.47	70.22	0.27	36.71
D_{tot}	[-]	0.0002	0.0008	0.4303	0.3290	0.0088

All damages are lower than 0.5 and most of them are very close to zero. The FAT value at 160 MPa for tension components is very high comparing of the stress ranges caused by the lorries. The stay breaking due to the fatigue is therefore not a major problem. This was expected because the stay in itself is not a favourable detail for fatigue phenomena. It would be better to verify a detail close to the anchorage with the main girder. The objective of this project being to determine λ factors for critical length higher than 80m, damages should be compared even if those are very low. We seek a match in damages to see if the fatigue verification procedures are adequate.

7.3. Conclusions

As for bottom flange elements, damages according to the FLM3 have to be calculated using the relation (6.5). Results are described in the following table:

Table 14 : Comparison damages for stays

			L16	L11	L1	C1	C16
FLM3	λ	[-]	2.69	2.69	2.26	2.26	2.26
	D_{tot}	[-]	0.0039	0.0102	0.4704	0.3707	0.0185
FLM4	D_{tot}	[-]	0.0002	0.0008	0.4303	0.3290	0.0088

First, the total damages according to FLM4 are close to those calculated with FLM3. This is a different conclusion than the one of fatigue procedures for bottom flange elements. Indeed, total damages of the bottom flange elements are multiplied by 5 or 8 between FLM3 and FLM4.

As has already been said, damages are calculated with a FAT value of 160 MPa and this value is largely higher than the stress ranges caused by the FLM4 lorries. The stays are also design in such a way that only 50% of their resistance are used. Considering this, the very low value of total damages is more understandable.

Damage equivalent factor method for critical lengths higher than 80m has different conclusions than for well-known critical lengths. Moreover, fatigue resistance is satisfied for all results. However, it is not possible to affirm that the constant trend of the λ factor for critical length higher than 80m without more researches. Indeed, although hypotheses made on the Maddah researches [5] have satisfactory outcome, it would be better to determine new damage equivalent factors based on a "real traffic" such as the *Fatigue load model 5*. It would be able to compare them with the hypotheses.

8. Comparison of damage equivalent factors

The objective of this last chapter is to perform the method of Hirt (Figure 2.4 [3]) in order to determine new λ factors for critical lengths higher than 80m. This method is based on the Figure 2.4 and consists of calculating a stress range with a load model (usually FLM3) and an equivalent stress range at 2×10^6 cycles with a total damage of 1.0, using a “real traffic” with FLM5. The division between these two stresses gives us the damage equivalent factor, as described in the following relation:

$$\lambda = \frac{\Delta\sigma_{E,2}}{\Delta\sigma(Q_{fat})} \quad (8.1)$$

In this project, there are a lot of data and influence lines on which we can work on. However, it has been decided to focus first on the central stays because they have an easy influence line with critical lengths higher than 80m. Knowing that this stay’s type is common in the most of cable-stayed bridge, this choice is a relevant one to understand the behaviour of λ factors for unknown critical lengths.

The different parts of this chapter explain how it is possible to determine the different stress ranges using in the λ factor calculations for one stay and then to present the final results. The selected stay is the central one C9, which has average characteristics.

8.1. Resulting from code load model

First of all, the stress range according to the model must be calculated. The model used is FLM3 (Figure 2.8), which is described in the first chapter based on the EN 1991-2 [12]. This stress range is determined using a main lorry with a total load of 480 kN and a second lorry with a load of 144 kN (4 axes of 36 kN instead of 120 kN) at a distance of 40m. The second vehicle has the same geometry of the main one.

These vehicles move on the influence line in order to obtain the maximum and minimum stress caused by them. The obtained results are showed in the following table:

Table 15 : Stress range from load model

Type of section			Midspan
Critical length	L_{crit}	[m]	129
Area	A	[m ²]	0.007193
Distance	D	[m]	40
Fatigue load Q_1	$Q_{fat,1}$	[kN]	480
Fatigue load Q_2	$Q_{fat,2}$	[kN]	144
Minimal stress	$\sigma_{min}(Q_{fat})$	[MPa]	-1.40
Maximal stress	$\sigma_{max}(Q_{fat})$	[MPa]	31.64
Stress range	$\Delta\sigma(Q_{fat})$	[MPa]	33.04

8.2. Resulting from service loads

The methodology to determine the stress range from service loads is described in the left part of the Figure 2.4. As the fatigue detail and the influence line are already found, a “real traffic” must be generated. The software used to do that is *MatLab developed by MathWorks and allows matrix manipulation, plotting of functions and data and implementation of algorithms*⁸.

Because of time, there are no extensive researches on the definition of a “real traffic”. It has been decided to generate a traffic based on the lorries of the FLM4. Thus, the model used is a kind of simplified FLM5 composed by six different vehicles, which are a normal vehicle with a load of 0 kN and the five lorries of FLM4 with the associated load. Moreover, it has been also decided to consider 25% of the heavy vehicles in the traffic. With the help of the software *MatLab*, it is possible to generate a uniform probability and then choose randomly a vehicle between all of them with the constraint that 25% of these vehicles are heavy vehicles.

$Q_0 = 0 \text{ kN}$	$Q_1 = 200 \text{ kN}$	$Q_2 = 310 \text{ kN}$	$Q_3 = 490 \text{ kN}$	$Q_4 = 390 \text{ kN}$	$Q_5 = 450 \text{ kN}$
25% of heavy vehicles (HV)					

The second required parameter is the distance. Indeed, a distance has to be define between each vehicle generated. To do so, the PhD thesis of Claudio Baptista (Baptista, 2016) [13] has been taken as an inspiration. Still using the software *MatLab*, it is possible to generate randomly a uniform probability and then, with the inverse function of the CDF curve, to determine a distance between each vehicle. The CDF curve is the *Cumulative Distribution Function* curve and it is based on the PDF (*Probability Distribution Function*) curve. The parameters of the CDF curve are taken from the PhD thesis of Claudio Baptista [13] and are:

$$f(p) = \text{gaminv}(p, \alpha, \beta) \quad (8.2)$$

$$d_0 = 120 \text{ m} \rightarrow \text{mean value}$$

$$d_m = 30 \text{ m} \rightarrow \text{modal value}$$

$$\alpha = \frac{d_0}{d_0 - d_m} = 1.33 \quad (8.3)$$

$$\beta = d_0 - d_m = 90 \text{ m}$$

The distance between the vehicles is based on a *Gamma distribution* for free-flow conditions [13]. With the following figures, it is possible to see the probability of having a distance (Figure 8.1) and how many time a distance has been generated in the traffic (Figure 8.2).

⁸ <https://en.wikipedia.org/wiki/MATLAB>

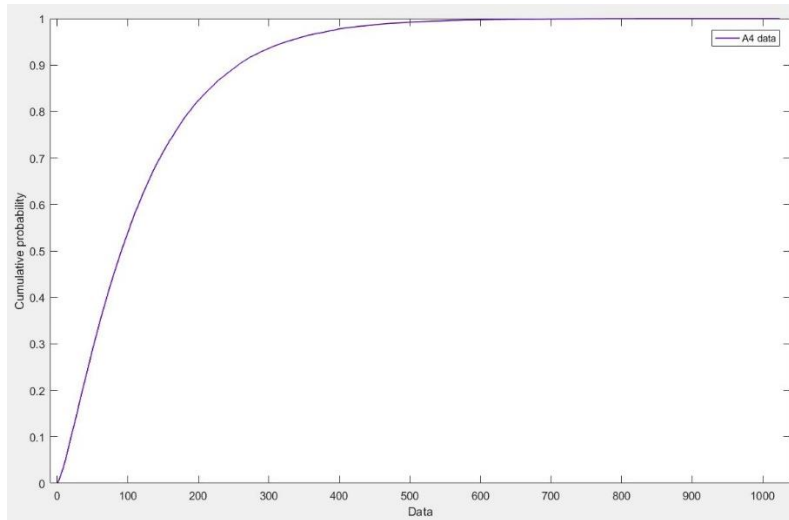


Figure 8.1 : CDF curve (from the software *MatLab*)

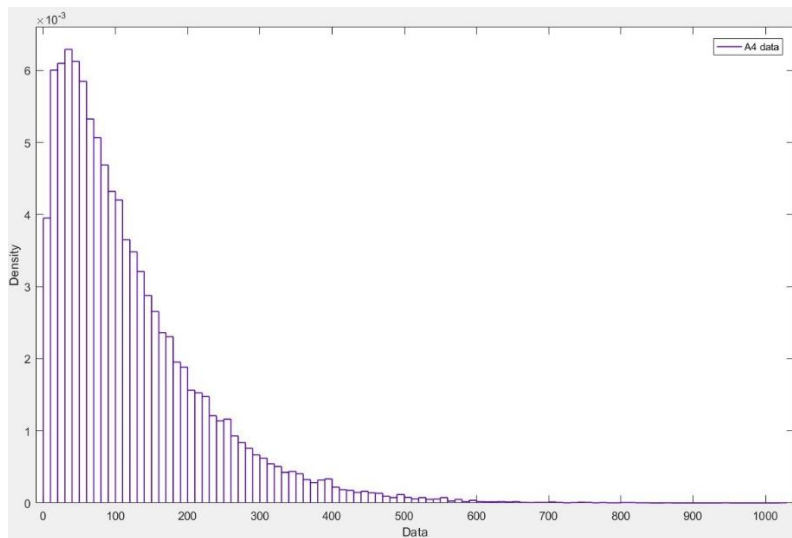


Figure 8.2 : PDF curve (from the software *MatLab*)

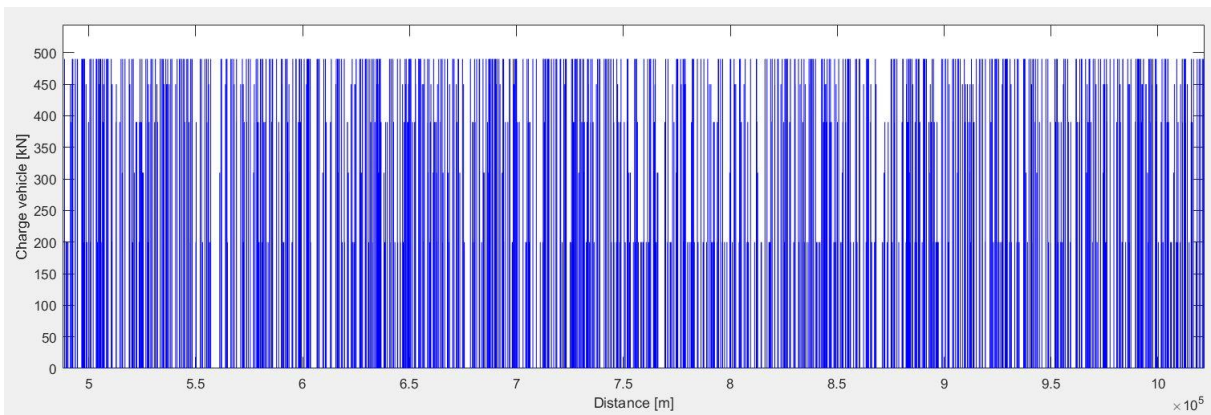


Figure 8.3 : Traffic generated (from the software *MatLab*)

Now that the traffic composition is defined and also the distance between each vehicle, a traffic can be generated. Figure 8.3 shows us an example of a part of a generated traffic for one day. The number of vehicles for one day is 32'000 vehicles with 8'000 heavy vehicles. Indeed, it has been already specified that the model considered $N_{obs} = 2 \times 10^6$ HV/year/lane for one traffic lane. Knowing that the traffic composition takes into account 25% of heavy vehicles and knowing that there are 250 working days per year, the number of vehicles per working day is:

$$\frac{4 \cdot 2 \cdot 10^6}{250} = 32000 \text{ veh/day} \tag{8.4}$$

Calculations will be first made with one-day data, then a comparison will be made with one-week data and one-year data. The numbers of cycles obtained are multiplied in order to consider a bridge's working life of 100 years. As an example, if we use one-day data, we have to multiply by 250 working days and by 100 years.

In the Figure 8.3, it is possible to see each vehicle from the line at 490 kN to the one at 200 kN and the blank spaces are the light vehicles with a load of 0 kN. As the traffic is generated, the different stress ranges caused by it can be calculated. To do so, the traffic must move on the influence line of the stay C9 to obtain the stress history and then it is possible to perform the "Rainflow" method to obtain a histogram.

Figure 8.4 represents the histogram for one-day data for the stay C9. The histogram represents the number of cycles for each stress range caused by the traffic. We can notice that there is a peak (for 30 MPa) that is equal to about 50% of the total number of cycles. This is because the vehicle 3 with a load of 490 kN represents 50% of the heavy traffic, according to the traffic type considered is *long distance*.

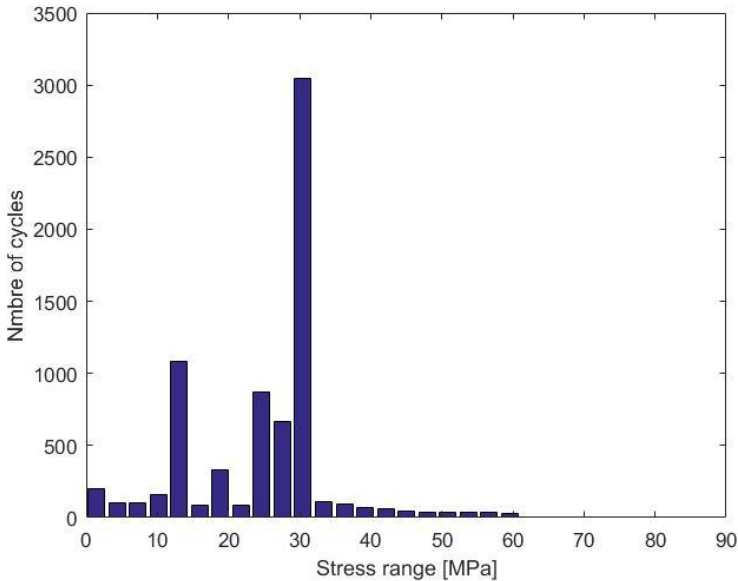


Figure 8.4 : Histogram for one-day data of stay C9

Finally, it is possible to determine the equivalent stress at 2×10^6 cycles in order to calculate the new λ factor. Because all calculations are made for stays, the S-N curve is based on the Figure 2.3, which considers slope's coefficient of 4 and 6 separated by the FAT value at 2×10^6 cycles. Thus, the FAT value corresponds to the desired stress. To determine it, the damage accumulation method must be performed with the constraint that total damages are equal to 1.0, as described in the following relations:

$$D_i = \frac{n_i}{N_{Ri}} = \frac{\Delta\sigma_i^m \cdot n_i \cdot 250 \cdot 100}{FAT^m \cdot 2 \cdot 10^6} \quad (8.5)$$

$$D_{tot} = \sum_i D_i = 1 \quad (8.6)$$

Here, $\Delta\sigma_i$ corresponds to the stress ranges described in the histogram and n_i corresponds to the number of cycle associated at each of these stress ranges. The m coefficient varies between 4 and 6 according to the considered stress range. Indeed, if it higher than the FAT value then the slope's coefficient is equal to 4 and if not, the m coefficient is equal to 6.

Using the software *MatLab*, a *while* loop is created, which allows to vary the FAT value until the total damages are equal or close to 1.0. The obtained results for the stay C9 are summarized in the following table:

		C9
FAT	[MPa]	70
D_{tot}	[-]	1.0546

Table 16 : Obtained results for one-day data of the stay C9

Knowing the two stress variations, we can perform the relation (8.1) as follows:

$$\lambda = \frac{FAT}{\Delta\sigma(Q_{fat})} = \frac{70}{33.04} = 2.12 \quad (8.7)$$

As explained previously, this λ factor is based on one-day data, which represents 32'000 vehicles with 8'000 HV. However, this value cannot represent the same as one-year traffic data. For some IT performances, it has been generated one-week traffic data, which represents 160'000 vehicles (for five working days) with 40'000 HV. The histogram and the obtained values are described in the next figure and table:

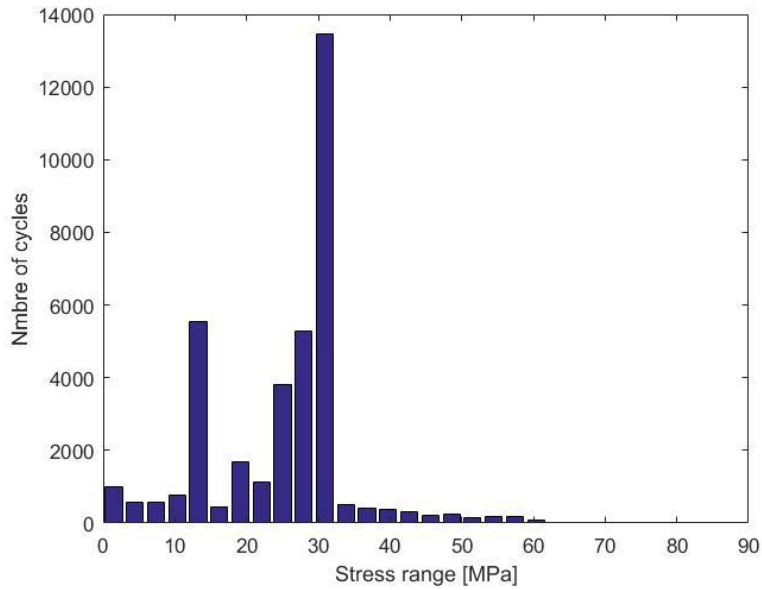


Figure 8.5 : Histogram for one-week data of stay C9

		C9
$\Delta\sigma(Q_{fat})$	[MPa]	33.04
FAT	[MPa]	69
D_{tot}	[-]	1.0445
λ	[-]	2.09

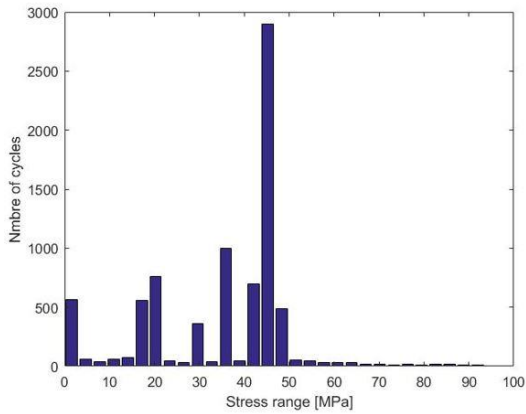
Table 17 : Obtained results for one-week data of the stay C9

We have to be careful because the relation (8.5) must be slightly adjusted. Indeed, these calculations are based on one-week data, so we have to modify the factor 250 by 50. We notice that the obtained values are very close. Moreover, by comparing the Figure 8.4 and the Figure 8.5, we can see that the histograms have a similar shape. Hence, we may deduce that the one-day traffic data can be enough in order to determine the new damage equivalent factors.

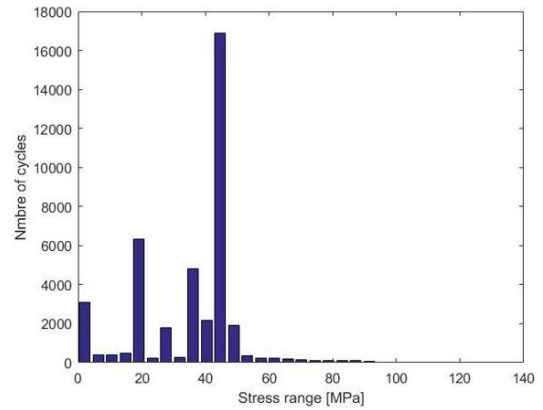
In this context, it is possible to apply this comparison to some other stays with different critical lengths and influence lines. The selected stays are taken from the central stays and are:

C1	C5	C13
$L_{crit} = 89m$	$L_{crit} = 105m$	$L_{crit} = 150m$

The comparisons are showed in the following figures. The left part represents the traffic data and obtained values for one day and the right part for one week.

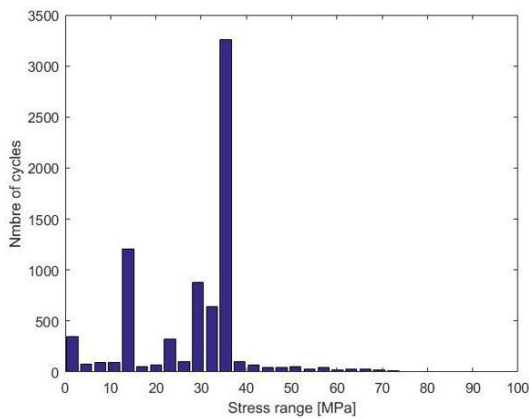


$\Delta\sigma(Q_{fat})$	=	48.73 MPa
FAT	=	99 MPa
D_{tot}	=	1.0462
λ	=	2.03

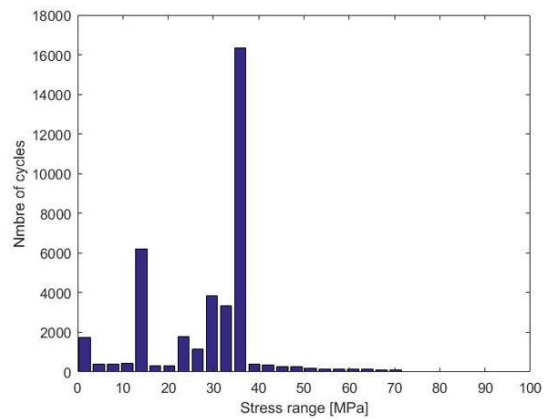


$\Delta\sigma(Q_{fat})$	=	48.73 MPa
FAT	=	101 MPa
D_{tot}	=	1.0046
λ	=	2.07

Figure 8.6 : One-day data vs one-week data of stay C1

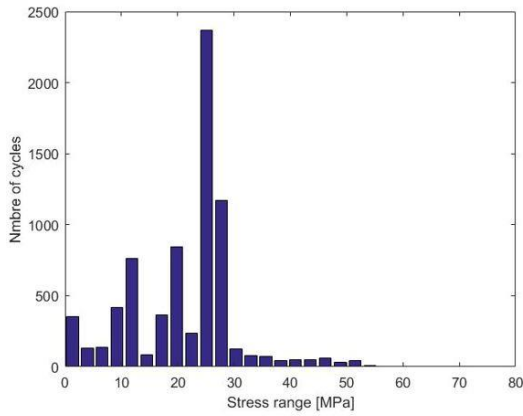


$\Delta\sigma(Q_{fat})$	=	38.1 MPa
FAT	=	81 MPa
D_{tot}	=	1.0011
λ	=	2.13

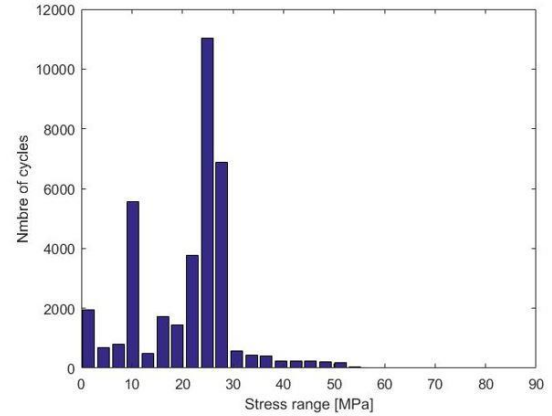


$\Delta\sigma(Q_{fat})$	=	38.1 MPa
FAT	=	81 MPa
D_{tot}	=	1.0060
λ	=	2.13

Figure 8.7 : One-day data vs one-week data of stay C5



$\Delta\sigma(Q_{fat})$	=	29.15 MPa
FAT	=	62 MPa
D_{tot}	=	1.0848
λ	=	2.13

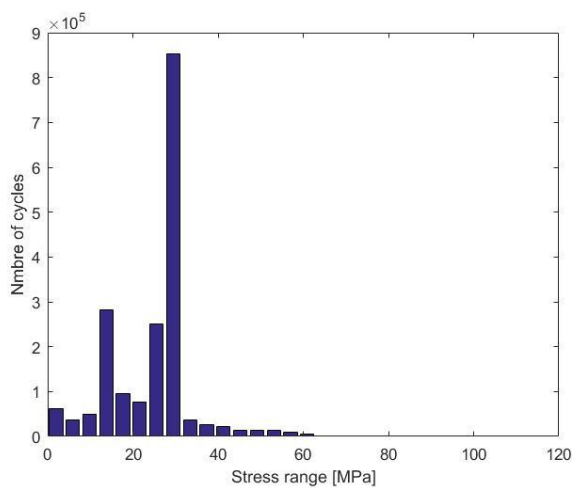


$\Delta\sigma(Q_{fat})$	=	29.15 MPa
FAT	=	62 MPa
D_{tot}	=	1.0604
λ	=	2.13

Figure 8.8 : One-day data vs one-week data of stay C13

First, the histograms and the obtained values are similar for each stays. It is true that there are some little differences but the peaks that characterise these histograms are presents for the same stress ranges. Thus, using one-day traffic data to generalize calculations (Q_{fat}) may be considered as reasonable.

To confirm this conclusion, Figure 8.9 show the results for one-year data of stay C9. They are similar to the one-day and one-week data.



$\Delta\sigma(Q_{fat})$	=	33.04 MPa
FAT	=	69 MPa
D_{tot}	=	1.0859
λ	=	2.09

Figure 8.9 : One-year data of stay C9

8.3. Damage equivalent factor

Thus, we have results for four stays with an identical influence line but with different critical lengths. Those vary between 89m and 150m that allows to have a good idea of the λ factors trend for critical lengths higher than 80m. The results are summarized in the following table:

		C1	C5	C9	C13
L_{crit}	[m]	89	105	129	150
FAT	[MPa]	99	81	70	62
$\Delta\sigma(Q_{fat})$	[MPa]	48.73	38.1	33.04	29.15
λ	[-]	2.03	2.13	2.12	2.13

Table 18 : λ factors for the stays C1, C5, C9 and C13

The first observation is that λ factors values are equals in average around 2.1 (the exact average is $\lambda_{moy} = 2.1025$). This should give us confidence that the trend is constant for critical lengths higher than 80m, which was the hypothesis based on the PhD thesis of Nariman Maddah [5] for the first calculations.

In order to consolidate these results, it would be effective to compare them with the values from the Eurocodes and the ones based on the Maddah's researches. The obtained results in this project are calculated for a heavy traffic of 2×10^6 HV/year/lane for one traffic lane.

Knowing that the Eurocodes are based on a heavy traffic of 5×10^5 HV/year/lane, we must multiply the partial factor λ_1 by λ_2 ($\lambda_2 = 1.2233$). We do not take into account the partial factors λ_3 and λ_4 because they are equals to 1.0. Assuming the hypothesis that λ_1 is constant for critical lengths higher than 80m, the Eurocodes give us for a midspan section the next value:

$$\lambda = 1.85 \cdot 1.2233 \approx 2.26 \quad (8.8)$$

To determine the value according to the researches of Nariman Maddah, it is possible to use the Figure 7.1 for a midspan section. The average value for the damage equivalent factor is equal to about 2.0. As the PhD thesis of Nariman Maddah [5] is based on a heavy traffic of 5×10^5 HV/year/lane, we can calculate:

$$\lambda = \lambda_{moy} \cdot \lambda_2 = 2.0 \cdot 1.2233 \approx 2.45 \quad (8.9)$$

We can summarize these results in a table and plot them in a graph for illustrating.

		C1	C5	C9	C13
λ (Matlab)	[-]	2.03	2.13	2.12	2.13
λ (Eurocodes)	[-]	2.26	2.26	2.26	2.26
λ (Maddah)	[-]	2.45	2.45	2.45	2.45

Table 19 : Comparison of λ factors for C1, C5, C9 and C13

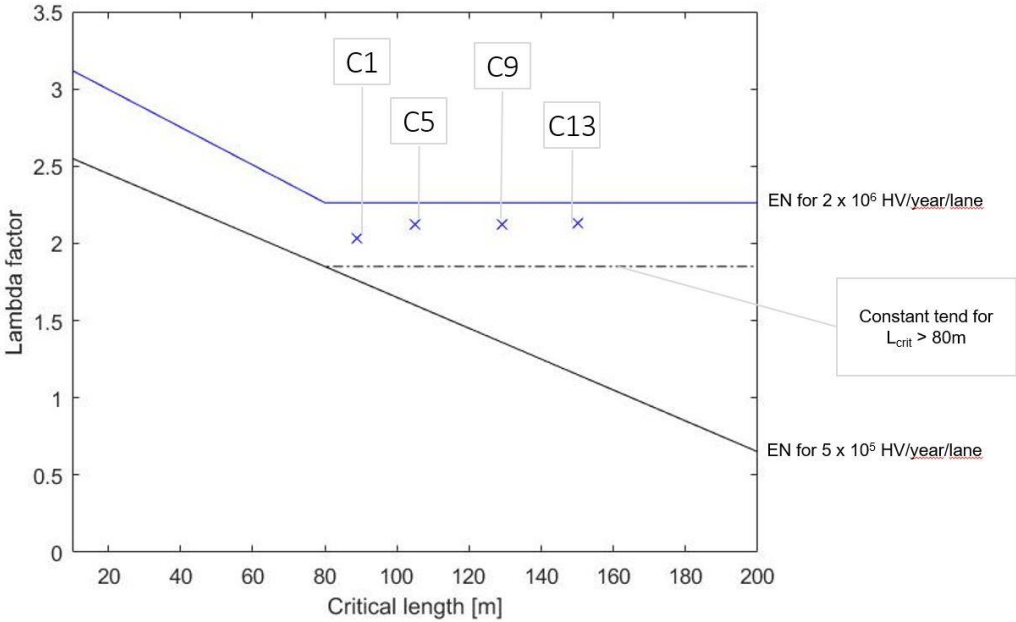


Figure 8.10 : Comparison of λ factors for C1, C5, C9 and C13

On Figure 8.10, the constant trend of λ factors is clearly visible. We can also notice that all calculated values are lower than those from the Eurocode and those from the Maddah’s thesis too. Thus, the following question can be asked: “Why do I obtain lower results than the Eurocodes ones when the results of Maddah’s thesis are higher?”

The answer comes from the only different element of the calculations: the fatigue curve used. Indeed, in this project, the stays are analysed. They are considered as tension components and thus, the S-N curve used is based on the slope’s coefficients equal to 4 and 6 without cut-off limit. But for the calculations of the Maddah’s thesis, the S-N curve used is based on the coefficients equal to 3 and 5 with a cut-off limit.

This difference, which is mainly occurred in the damage accumulation, allows to explain these lower values. However, another question can be asked: “If there is a difference in the calculations of the λ factor considering the fatigue curves and the slope’s coefficients, are formulas and values still valid for the fatigue verifications for stays?”

Indeed, the partial factors λ_1 and λ_2 are based on tests made with elements using fatigue curves for steel members, as described in the Figure 2.2. Leaving out the partial factor λ_1 for now, we can focus on λ_2 . The Eurocodes (EN 1993-2 [8]) give us a formula for calculating λ_2 , taking into account a m coefficient equal to 5. Trying to adjust the relation for stays, we can use a m coefficient of 6 to obtain:

$$\lambda_2 = \frac{Q_{m1}}{Q_0} \left(\frac{N_{obs}}{N_0} \right)^{1/6} = 1.1681 \tag{8.10}$$

Thus, as a first approximation, the Eurocodes values are slightly adjusted by multiplying them by the adjusted partial factor. In order to better understand the different uses of these fatigue curves, damage accumulation has been calculated for the both S-N curves. In the Figure 8.12, the differences are illustrated. In blue, formulas and calculations have been made according to the slope's coefficients of 3 and 5, taking into account a cut-off limit. In red, formulas and calculations for coefficients of 4 and 6 without cut-off limit.

Moreover, some lateral stays have been considered in order to have more data to compare. However, only those which have a midspan section to compare the appropriate values for the λ factor. Using the adjusted partial factor λ_2 , it is possible to calculate the λ factor value for slopes equal to 4 and 6, according to the Maddah's results. In the following table, all data of the Figure 8.12 are summarized:

N°	L _{crit} [m]	$\lambda_{3,5}$	$\lambda_{4,6}$
L12	54	2.32	2.00
L14	54	2.38	2.05
L7	71	2.63	2.25
L9	71	2.38	2.02
L3	81	2.24	1.94
L1	89	2.25	1.95
C1	89	2.34	2.03
C5	105	2.44	2.13
C9	129	2.27	2.12
C13	150	2.37	2.13
λ (Eurocode)		2.26	2.16
λ (Maddah)		2.45	2.34
Average		2.33	2.04

Table 20 : λ factors for m=3,5 and m=4,6

In conclusion, it should be confirmed (in future works) that the λ factor values are slightly lower for the calculations with slope's coefficients of 4 and 6 and slightly higher for those with coefficients of 3 and 5.

Moreover, the value of the lateral stay L7 is much higher than the others due to the approximation of its influence line with the software MatLab has been bad made. Figure 8.11 show us the comparison

between the real influence line (in red) and the approximation (in blue). One can notice that even if the general shape is kept, the maximal peak value and the minimal one are not reached. For this reason, the lateral stay L7 is not taken into account for calculations of the average.

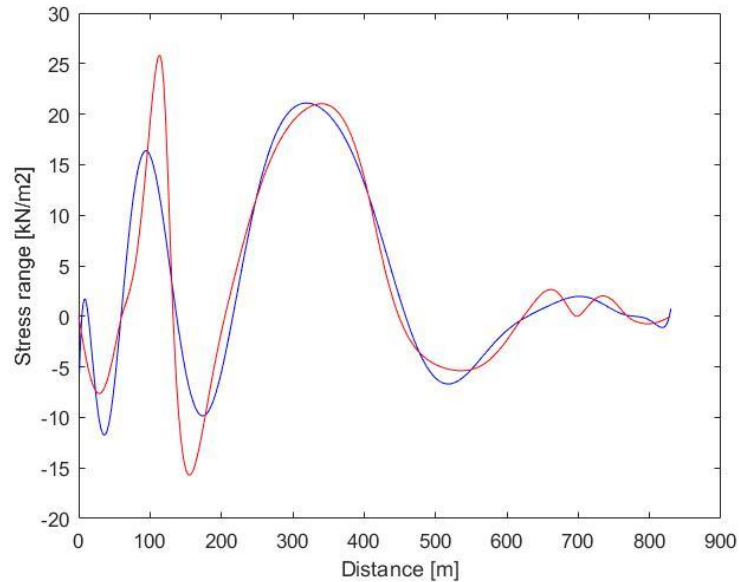


Figure 8.11 : Approximation of the lateral stay L7

Concerning the Figure 8.12, we notice clearly that the λ factors have a constant trend for critical length which vary from 54m to 150m for influence lines with a midspan section shape. This is not only to confirm hypotheses calculations of this project, which support the results of the Maddah's thesis, but also to ask questions about the value of the damage equivalent factor described in the Eurocodes.

Indeed, taking into account of the results of the Maddah's thesis and especially the ones of the Figure 7.1, we observe that the constant trend is visible for the critical lengths higher than 80m but also for the one lower than 80m, while the Eurocodes telling us to take a decreasing value.

Moreover, if the damage equivalent factor has a constant value for lengths varying from 54m to 150m, one can raise the question about the relevance of the critical length in the λ factor definition.

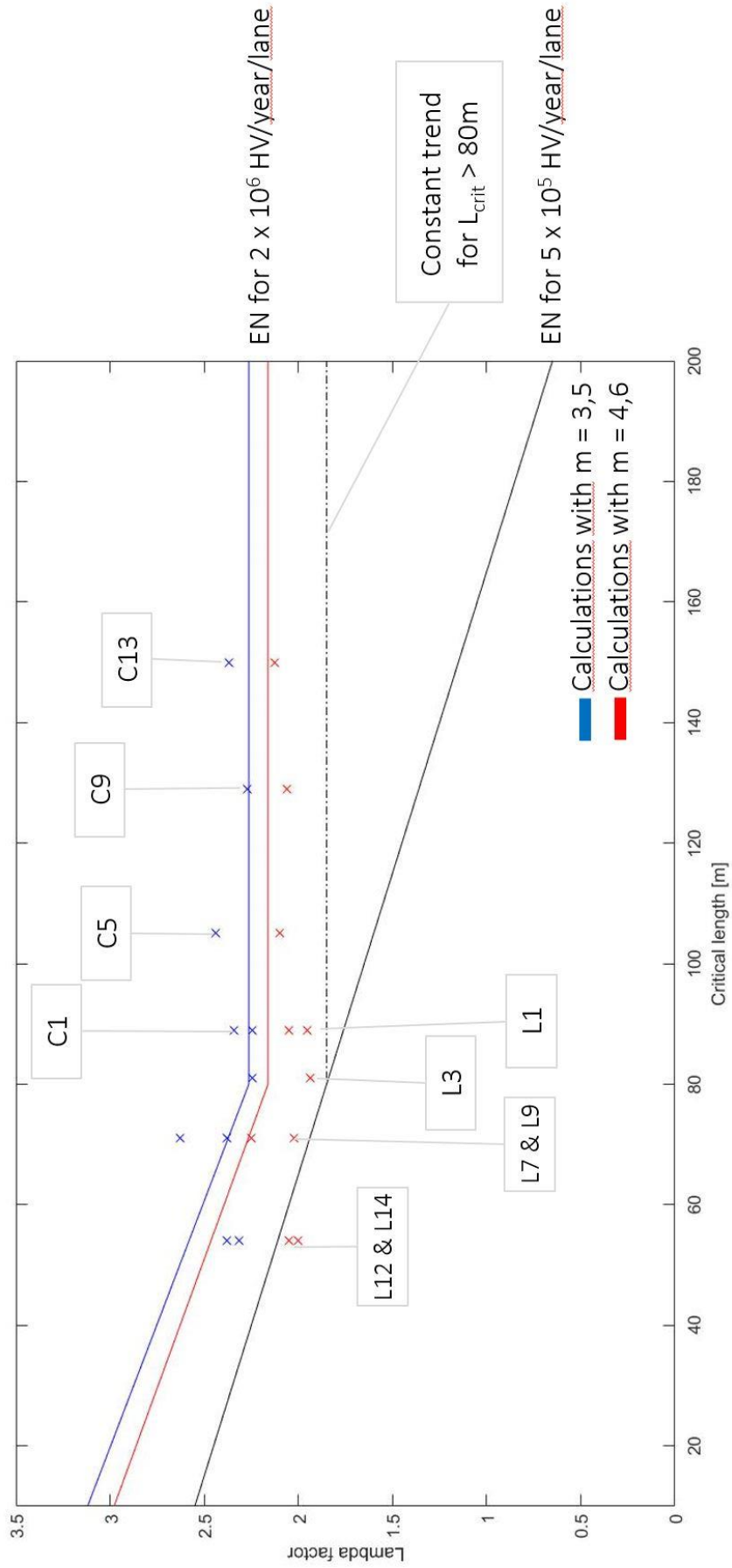


Figure 8.12 : Comparison λ factors with $m=3,5$ and $m=4,6$

9. Conclusions and future works

One of the most important goals of this Master thesis was to verify if the damage equivalent factor method could be used to structural systems such as cable-stayed bridges. The first objective was to determine the stress influence lines in order to take into account both the internal forces acting in the composite deck, namely the flexion and the compression. The second objective was to calculate the damage equivalent factor, noted λ , for critical length higher than the Eurocodes limit of 80m.

Based on these information, the idea is to propose an adjustment of the existing standard rules in order to perform fatigue verification procedure using λ factor for this kind of structural systems. This conclusion will be constructed around the two objectives presented previously and the adjustment of the existing rules. Taking into account the obtained results, it will be finally presented some recommendations for some futures researches on this topic.

9.1. Stress influence lines

The bending and the compression have different behaviour inside the structure and hence have different influence lines. However, the corresponding maximal and minimal efforts are not necessarily at the same location that means we have to define which one is the most decisive. To do so, the idea is to determine influence lines based on the total stresses calculated with the sum of the two internal forces stresses, as described in the equation (4.1). Moreover, the Figure 4.2 show that the stress based on the bending moment has more influence in the composite deck than the axial stress. In this fact, it is better to base the calculations on the maximal variation of the moments and add the associated variation of the axial forces to get the influence line which will better define the extreme stresses location.

It would be also interesting to study with more details the stays anchorage in the composite deck. Indeed, several internal forces act in this detail. Performing the same methodology, it will be possible to define stress influence lines for these details in order to know the extreme stresses locations.

9.2. Damage equivalent factor

Researches done during this Master thesis showed that damage equivalent factors for midspan section remain constant when the critical length increase, apart from slight variations. This observation may be considered as a support for the results of the PhD thesis of Nariman Maddah [5], as described in the Figure 7.1. But it was more surprising to see that this trend works also for lengths lower than the Eurocodes limit, although it is described in the Eurocodes that the λ factor linearly decreases when critical length increases. Results of this project and those of the Maddah's thesis suggest that the damage equivalent factor remains constant for lengths varying from 50m to 150m. Thus, this would allow to simplify fatigue verification procedures if it is not necessary to define the critical length.

It would be also interesting to determine the trend of λ factors for a section at support and to observe if the results match with the Maddah's researches too. Thus, it would be useful to define a fatigue verification procedure for tension components the fact that those elements are based on a different fatigue curve.

9.3. Adjustment of the existing standard rules

Taking into account long spans, one solution for the adjustment of the existing rules could be the next one. First, it would be better to define again the partial factor λ_1 for lengths varying between 20m and 200-300m. Then, it would be useful to define a new partial factor, noted λ_5 , which would allow for taking into account the type of the fatigue curve.

Indeed, knowing that the Eurocodes define several S-N curves with different slope's coefficients, it would be effective to have a factor taking into account these coefficients.

9.4. Future works

Regarding the future researches on this topic, I should like to say a few comments:

- In order to be more precise and close to the reality, a better traffic should be generated, as defined in the Eurocodes with the *Fatigue Load Model 5*. Moreover, using one-year traffic data would allow for supporting (or not) the results of this project.
- To complete this Master thesis, it would be great to perform the same calculations for influence line with a shape as a section at support with lengths between 20m and 200m.
- Develop researches to better understand the behaviour of damage equivalent factors according to the type of fatigue curve used. A better knowledge would perhaps make it possible to determine a partial factor λ_5 which would thus solve the slope's coefficients problems.

References

- [1] M. Virlogeux, "Les ponts à haubans. L'efficacité technique alliée à l'élégance architecturale," *Bull. Ponts Métalliques*, vol. 21, pp. 10–50, 2002.
- [2] M. A. Hirt, R. Bez, and A. Nussbaumer, *Traité de génie civil de l'École polytechnique fédérale de Lausanne. notions fondamentales et méthodes de dimensionnement Vol. 10, Vol. 10*,. Lausanne: Presses Polytechniques et Universitaires Romandes, 2001.
- [3] A. Nussbaumer, L. Borges, and L. Davaine, *Fatigue design of steel and composite structures: Eurocode 3: Design of steel structures, part 1 - 9 fatigue ; Eurocode 4: Design of composite steel and concrete structures*, 1. ed. Berlin: Ernst & Sohn [u.a.], 2011.
- [4] *Eurocode 3: Design of steel structures - Part 1-9: Fatigue*, Comité européen de normalisation CEN. Bruxelles, 2005.
- [5] N. Maddah, "Fatigue Life Assessment of Roadway Bridges based on Actual Traffic Loads," Ecole Polytechnique Fédérale de Lausanne, Lausanne, 2013.
- [6] *Eurocode 3 - Design of steel structures - Part 1-11: Design of structures with tension components*, Comité européen de normalisation CEN. Bruxelles, 2006.
- [7] C. R. Hendy and D. A. Smith, *Designers' guide to EN 1993-2: Eurocode 3: design of steel structures: part 2: steel bridges*, Repr. 2010. London: Thomas Telford, 2007.
- [8] *Eurocode 3 - Design of steel structures - Part 2: Steel Bridges*, Comité européen de normalisation CEN. Bruxelles, 2006.
- [9] *Eurocode 1: Actions on structures - Part 2: Traffic loads on bridges*, Comité européen de normalisation CEN. Bruxelles, 2003.
- [10] J. J. Oliveira Pedro, "Pontes atirantadas mistas - Estudo do comportamento estrutural," Universidade Técnica de Lisboa - Instituto Superior Técnico, 2007.
- [11] SETRA, *Guidance book, Eurocodes 3 et 4, Application to steel-concrete composite road bridges*. Bagnex: Service d'études techniques des routes et autoroutes, 2010.
- [12] J.-A. Calgaro, M. Tschumi, and H. Gulvanessian, *Designer's guide to Eurocode 1: actions on bridges ; EN 1991-2, EN 1991-1-1, -1-3 to 1-7 and EN 1990 annex A2*. London: Telford, 2010.
- [13] C. Baptista, "Multiaxial and variable amplitude fatigue in steel bridges," Ecole Polytechnique Fédérale de Lausanne, Lausanne, 2016.
- [14] J. J. Oliveira Pedro and A. J. Reis, "Nonlinear analysis of composite steel–concrete cable-stayed bridges," *Eng. Struct.*, vol. 32, no. 9, pp. 2702–2716, Sep. 2010.
- [15] J. J. Oliveira Pedro and A. J. Reis, "Simplified assessment of cable-stayed bridges buckling stability," *Eng. Struct.*, vol. 114, pp. 93–103, May 2016.
- [16] J.-P. Lebet, M. A. Hirt, and C. Leonardi, *Ponts en acier: conception et dimensionnement des ponts métalliques et mixtes acier-béton*. Lausanne: Presses polytechniques et universitaires romandes, 2009.

Appendix 1

Case study details

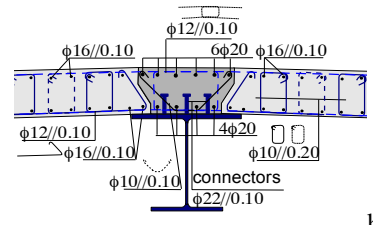
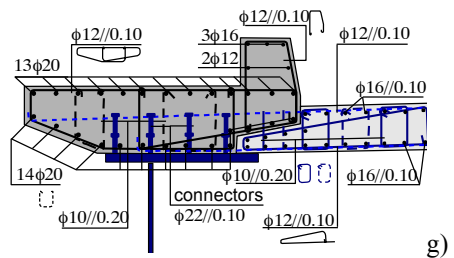
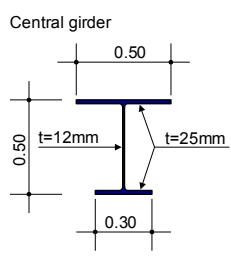
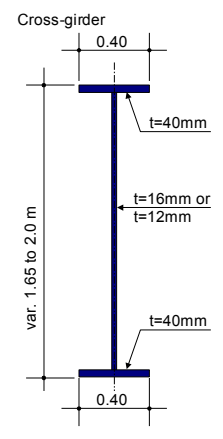
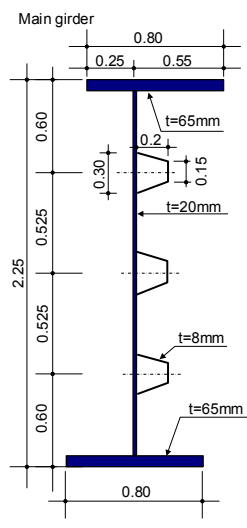
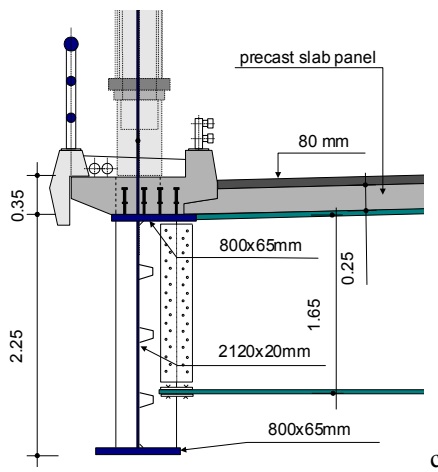
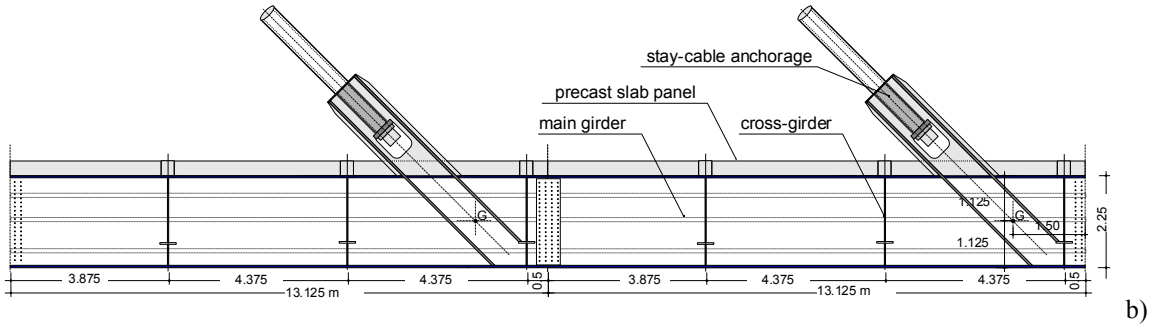
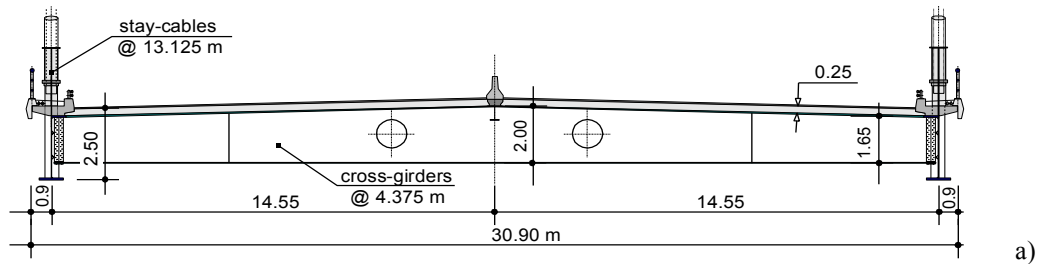
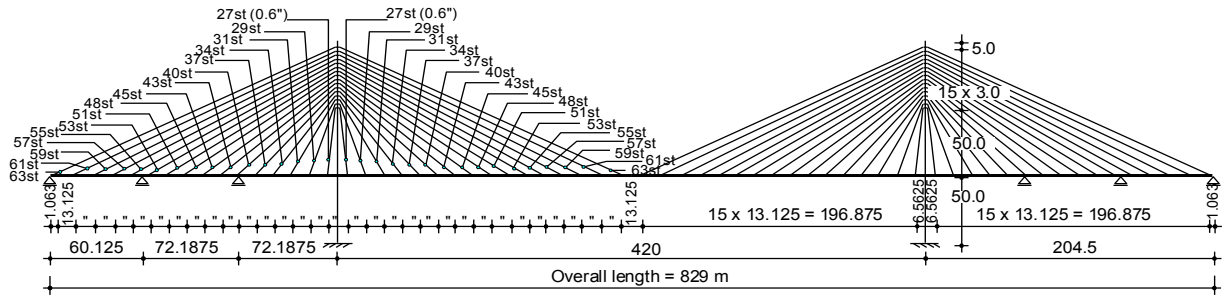


Fig. 2. Case study details: a) Longitudinal bridge arrangement and typical composite deck cross-section; b) longitudinal deck segments; c) cross-section of the main girders; d) cross-section of the main girders; e) cross-section of the cross-girders; f) cross-section of central girders; and g) slab reinforcement over the main girders; h) slab reinforcement over the central girders.

Appendix 2

Stays tensioning

Mise en tension - Haubans

cp_ep_lower

Installed forces

F_ha - F_cp

Factor f

Forces finales - TIR

Table with 2 columns: N° haubans, Forces [kN]. Rows 16L to 16C.

Table with 2 columns: N° haubans, Forces [kN]. Rows 16L to 16C.

Table with 2 columns: N° haubans, Forces [kN]. Rows 16L to 16C.

Table with 2 columns: N° haubans, Valeur. Rows 16L to 16C.

Table with 2 columns: N° haubans, Valeur. Rows 16L to 16C.

Load cases (ΔT = -1000°C)

Large data table with columns: Label - element, and various load case values (e.g., ΔT = -1000°C at 16L, 15L, etc.).

Matrice 32x32 inversée

Large matrix of numerical values, likely an inverse stiffness matrix, arranged in a grid.

Appendix 3

Simple influence lines from EN 1993-2 [7], article 9.5.2 (2), as follows:

(2) In determining λ_1 the critical length of the influence line or area may be taken as follows:

a) for moments:

- for a simply supported span, the span length L_i ;
- for continuous spans in midspan sections, see Figure 9.7, the span length L_i of the span under consideration;
- for continuous spans in support sections, see Figure 9.7, the mean of the two spans L_i and L_j adjacent to that support;
- for cross girders supporting stringers, the sum of the two adjacent spans of the stiffeners carried by the cross girder.

b) for shear for a simply supported span and a continuous span:

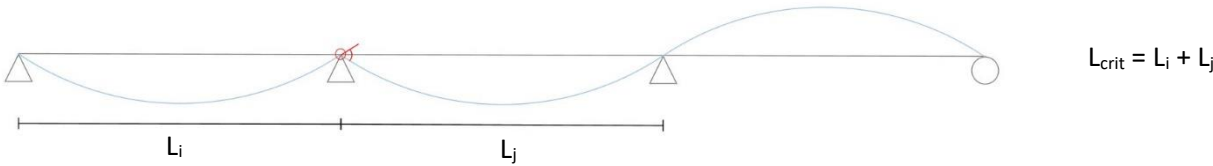
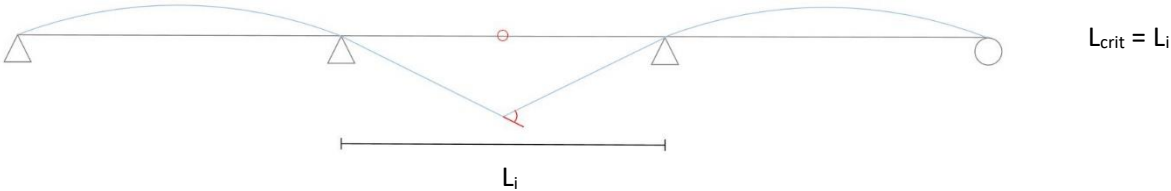
- for the support section, see Figure 9.7, the span under consideration L_i ;
- for the midspan section, see Figure 9.7, $0,4 \times$ the span under consideration L_i .

c) for reactions:

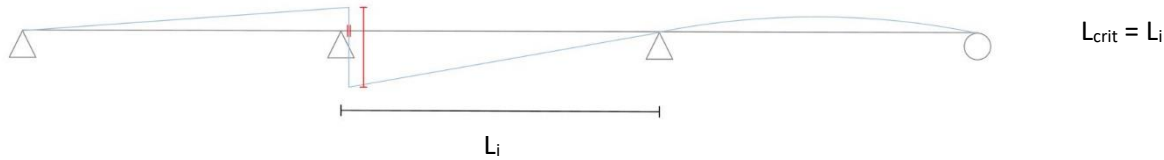
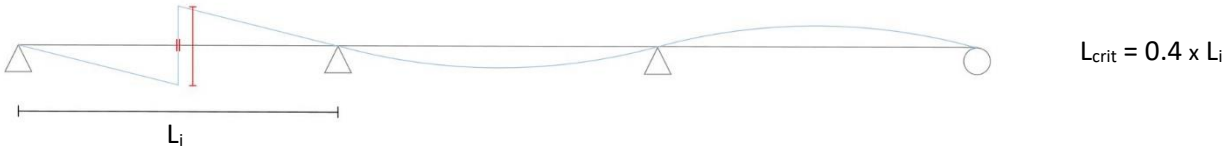
- for end support, the span under consideration L_i ;
- for intermediate supports, the sum of the two adjacent spans $L_i + L_j$.

Based on the EN 1993-2, article 9.5.2 (2)

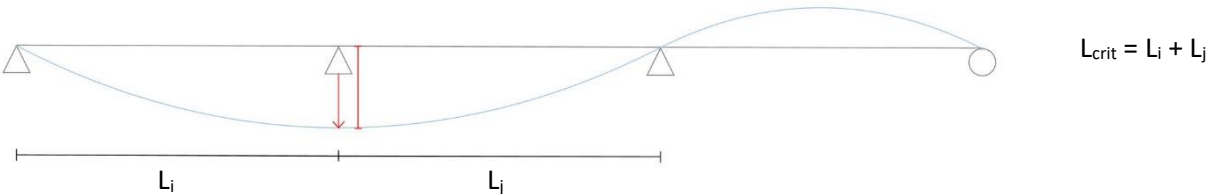
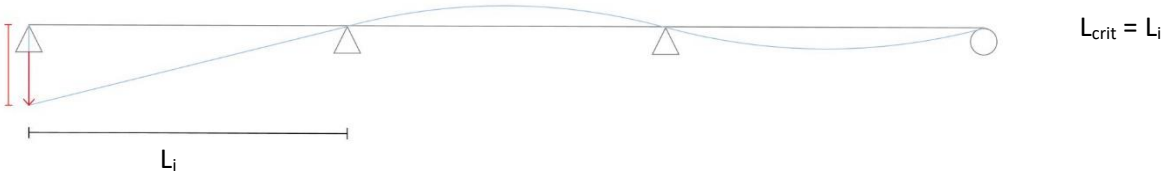
a) For moments: $\phi = 1$



b) For shear: $shear = 1$

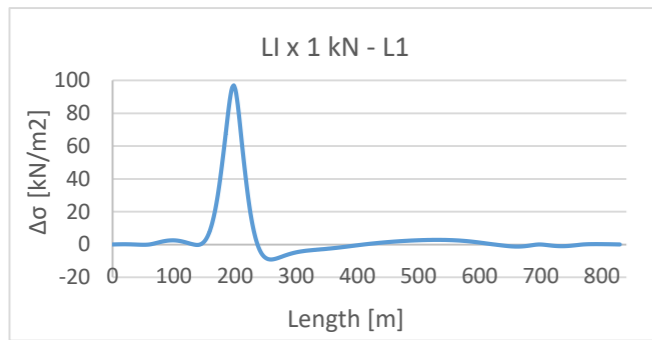


c) For reactions: $\delta = 1$

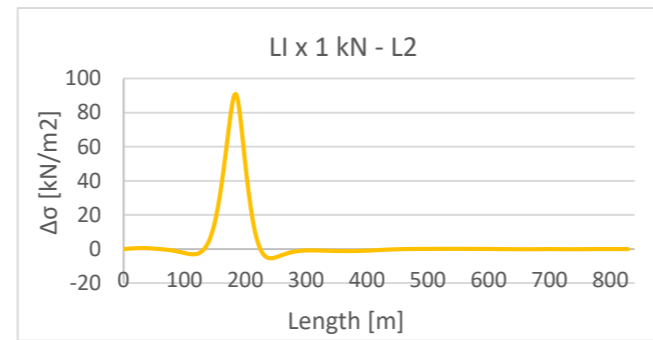


Appendix 4

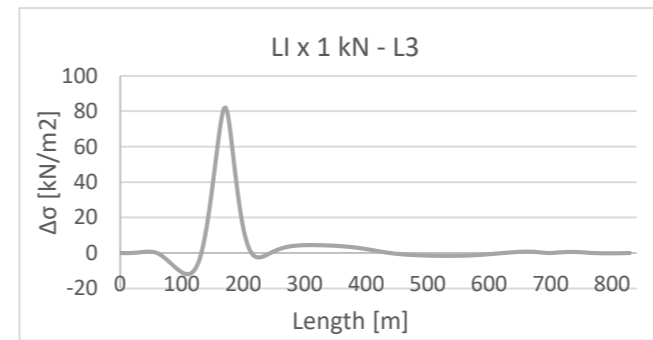
Influence lines of lateral stays



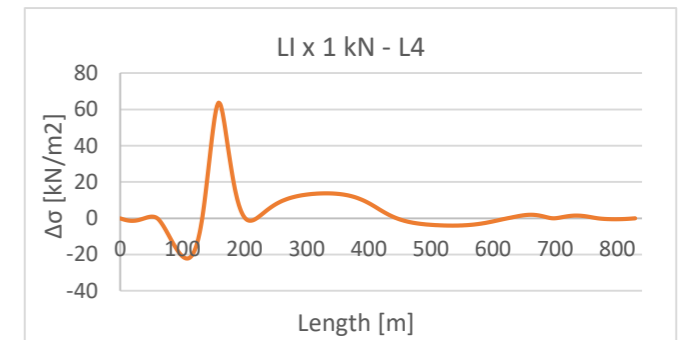
Moment – Midspan $L_{crit} = 89$ m



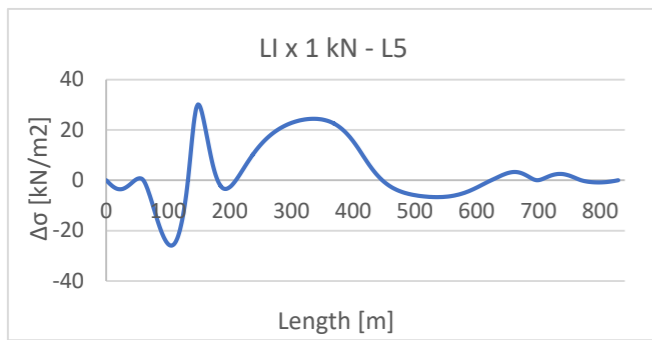
Moment – Midspan $L_{crit} = 100$ m



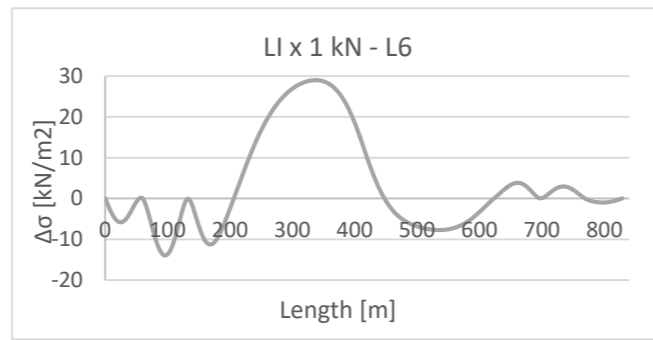
Moment – Midspan $L_{crit} = 81$ m



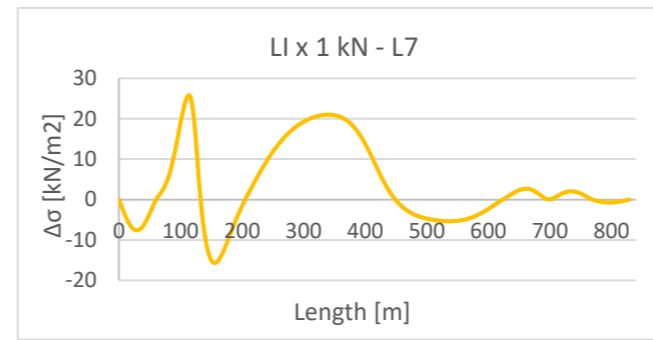
Moment – Support $L_{crit} = 315$ m



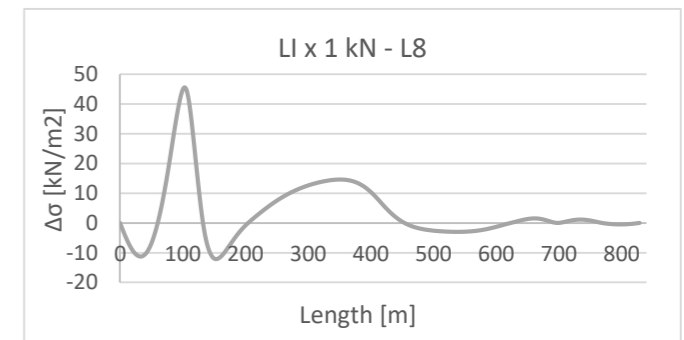
Moment – Support $L_{crit} = 315$ m



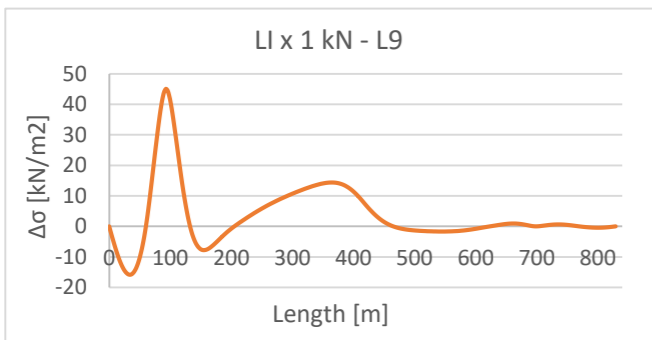
Moment – Support $L_{crit} = 145$ m



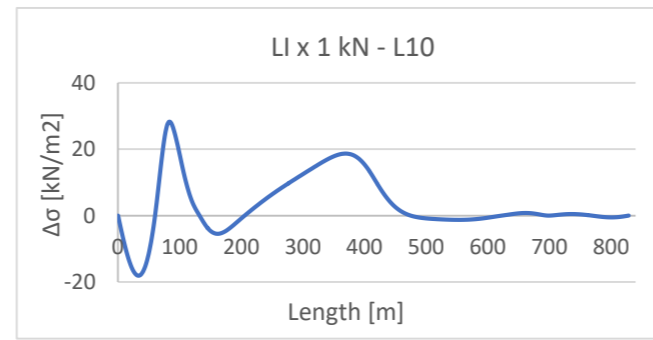
Moment – Midspan $L_{crit} = 71$ m



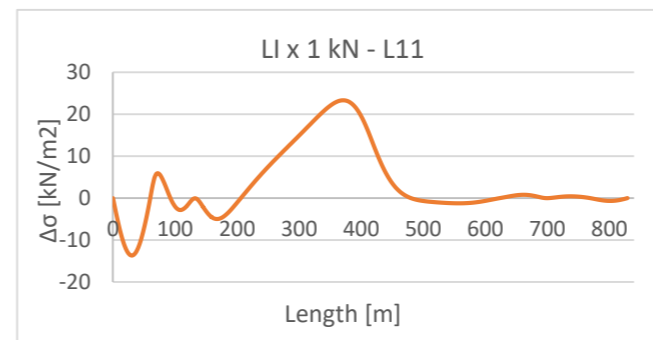
Moment – Midspan $L_{crit} = 71$ m



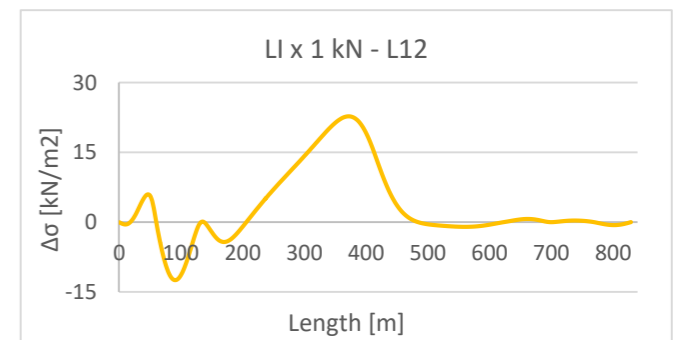
Moment – Midspan $L_{crit} = 71$ m



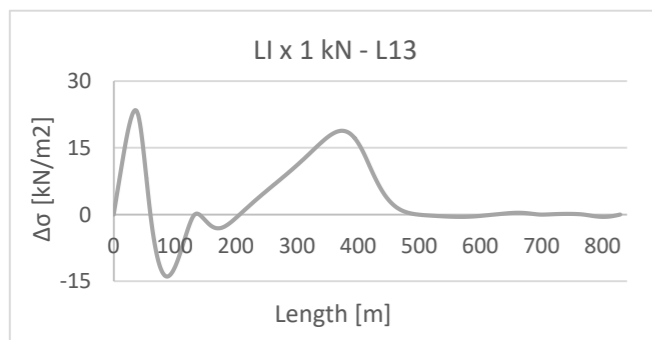
Moment – Midspan $L_{crit} = 71$ m



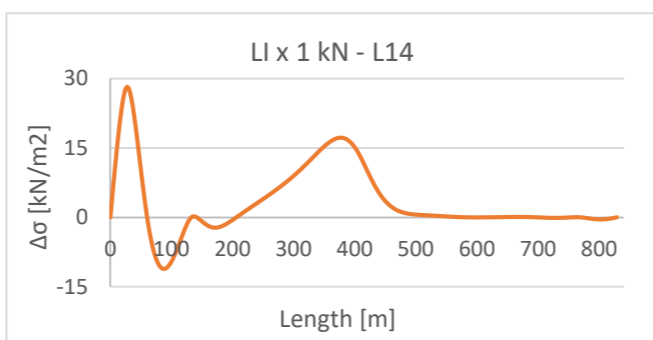
Support $L_{crit} = 100$ m



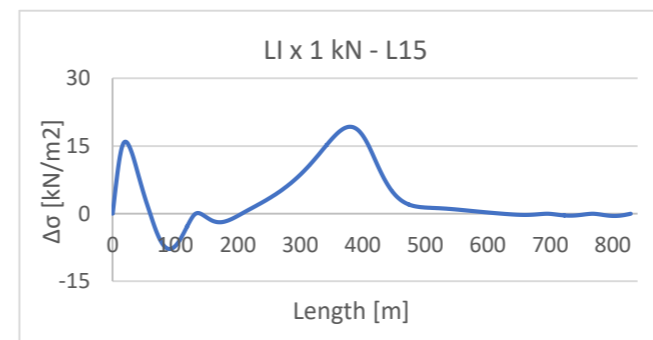
Moment – Support $L_{crit} = 140$ m



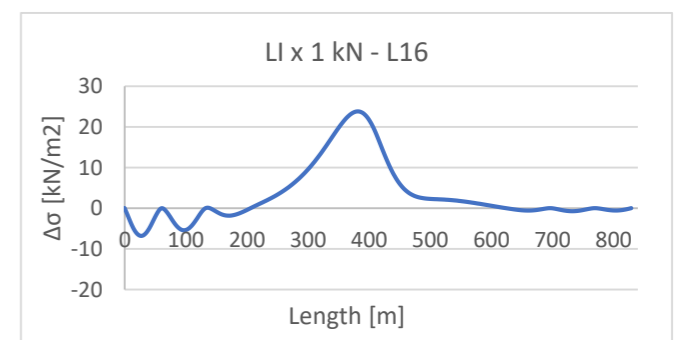
Shear – Midspan $L_{crit} = 54$ m



Shear – Midspan $L_{crit} = 54$ m



Shear – Midspan $L_{crit} = 54$ m



Moment – Support $L_{crit} = 135$ m

Appendix 5

Fatigue verification procedures for stays

Fatigue

		L16	L15	L14	L13	L12	L11	L10	L9	L8	L7	L6	L5	L4	L3	L2	L1
L_crit	[m]	135	54	54	54	140	100	75	75	75	75	145	315	315	85	100	89
λ₁	[-]	2.2	2.11	2.11	2.11	2.2	2.2	1.9	1.9	1.9	1.9	2.2	2.2	2.2	1.85	1.85	1.85
λ₂	[-]	1.22	1.22	1.22	1.22	1.22	1.22	1.22	1.22	1.22	1.22	1.22	1.22	1.22	1.22	1.22	1.22
λ₃	[-]	1.00	1.00	1.00	1.00	1.00	1.00	1.00	1.00	1.00	1.00	1.00	1.00	1.00	1.00	1.00	1.00
λ₄	[-]	1.00	1.00	1.00	1.00	1.00	1.00	1.00	1.00	1.00	1.00	1.00	1.00	1.00	1.00	1.00	1.00
λ	[-]	2.69	2.58	2.58	2.58	2.69	2.69	2.32	2.32	2.32	2.32	2.69	2.69	2.69	2.26	2.26	2.26
λ_{max}	[-]	2.70	2.00	2.00	2.00	2.70	2.70	2.00	2.00	2.00	2.00	2.70	2.70	2.70	2.00	2.00	2.00

λ	[-]	2.69	2.00	2.00	2.00	2.69	2.69	2.00	2.00	2.00	2.00	2.69	2.69	2.69	2.00	2.00	2.00
Δσ(Qfat)	[Mpa]	14.69	13.01	18.92	17.94	16.93	17.76	22.22	29.23	27.73	19.95	20.64	26.87	41.17	45.18	46.19	50.95
Δσ_{E,2*1.35}	[Mpa]	53.38	35.14	51.09	48.43	61.50	64.52	60.00	78.92	74.87	53.87	74.97	97.63	149.58	121.98	124.71	137.57
Δσ_c	[Mpa]	160.00	160.00	160.00	160.00	160.00	160.00	160.00	160.00	160.00	160.00	160.00	160.00	160.00	160.00	160.00	160.00
Vérification		OK	OK	OK	OK	OK	OK	OK	OK	OK	OK	OK	OK	OK	OK	OK	OK

		C16	C15	C14	C13	C12	C11	C10	C9	C8	C7	C6	C5	C4	C3	C2	C1
L_crit	[m]	162	162	160	150	150	145	130	125	100	100	100	90	90	90	90	89
λ₁	[-]	1.85	1.85	1.85	1.85	1.85	1.85	1.85	1.85	1.85	1.85	1.85	1.85	1.85	1.85	1.85	1.85
λ₂	[-]	1.22	1.22	1.22	1.22	1.22	1.22	1.22	1.22	1.22	1.22	1.22	1.22	1.22	1.22	1.22	1.22
λ₃	[-]	1.00	1.00	1.00	1.00	1.00	1.00	1.00	1.00	1.00	1.00	1.00	1.00	1.00	1.00	1.00	1.00
λ₄	[-]	1.00	1.00	1.00	1.00	1.00	1.00	1.00	1.00	1.00	1.00	1.00	1.00	1.00	1.00	1.00	1.00
λ	[-]	2.26	2.26	2.26	2.26	2.26	2.26	2.26	2.26	2.26	2.26	2.26	2.26	2.26	2.26	2.26	2.26
λ_{max}	[-]	2.00	2.00	2.00	2.00	2.00	2.00	2.00	2.00	2.00	2.00	2.00	2.00	2.00	2.00	2.00	2.00

λ	[-]	2.00	2.00	2.00	2.00	2.00	2.00	2.00	2.00	2.00	2.00	2.00	2.00	2.00	2.00	2.00	2.00
Δσ(Qfat)	[Mpa]	26.64	25.02	25.77	27.17	28.87	47.86	30.80	31.63	32.82	34.26	35.96	37.92	40.32	43.21	46.29	48.72
Δσ_{E,2*1.35}	[Mpa]	71.93	67.55	69.58	73.36	77.95	129.22	83.17	85.40	88.62	92.51	97.09	102.40	108.87	116.65	124.98	131.55
Δσ_c	[Mpa]	160.00	160.00	160.00	160.00	160.00	160.00	160.00	160.00	160.00	160.00	160.00	160.00	160.00	160.00	160.00	160.00
Vérification		OK	OK	OK	OK	OK	OK	OK	OK	OK	OK	OK	OK	OK	OK	OK	OK

Damages

		L16	L15	L14	L13	L12	L11	L10	L9	L8	L7	L6	L5	L4	L3	L2	L1
Δσ_C	[Mpa]	160.00	160.00	160.00	160.00	160.00	160.00	160.00	160.00	160.00	160.00	160.00	160.00	160.00	160.00	160.00	160.00
D_{tot}	[-]	0.0002	0.0001	0.0011	0.0008	0.0006	0.0008	0.0030	0.0153	0.0112	0.0016	0.0019	0.0093	0.1197	0.2091	0.2388	0.4303

		C16	C15	C14	C13	C12	C11	C10	C9	C8	C7	C6	C5	C4	C3	C2	C1
Δσ_C	[Mpa]	160.00	160.00	160.00	160.00	160.00	160.00	160.00	160.00	160.00	160.00	160.00	160.00	160.00	160.00	160.00	
D_{tot}	[-]	0.0088	0.0060	0.0072	0.0099	0.0142	0.0181	0.0210	0.0246	0.0307	0.0398	0.0532	0.0732	0.1057	0.1600	0.2419	0.3290